AD-A050 187 PENNSYLVANIA STATE UNIV UNIVERSITY PARK APPLIED RESE--ETC F/G 13/10
COMPUTER-ASSISTED DESIGN OF PUMP IMPELLERS.(U)
JAN 78 M C BROPHY N00017-73-C-1418
TM-7A-02 NL

UNCLASSIFIED

1 OF 2

AD
A050 187

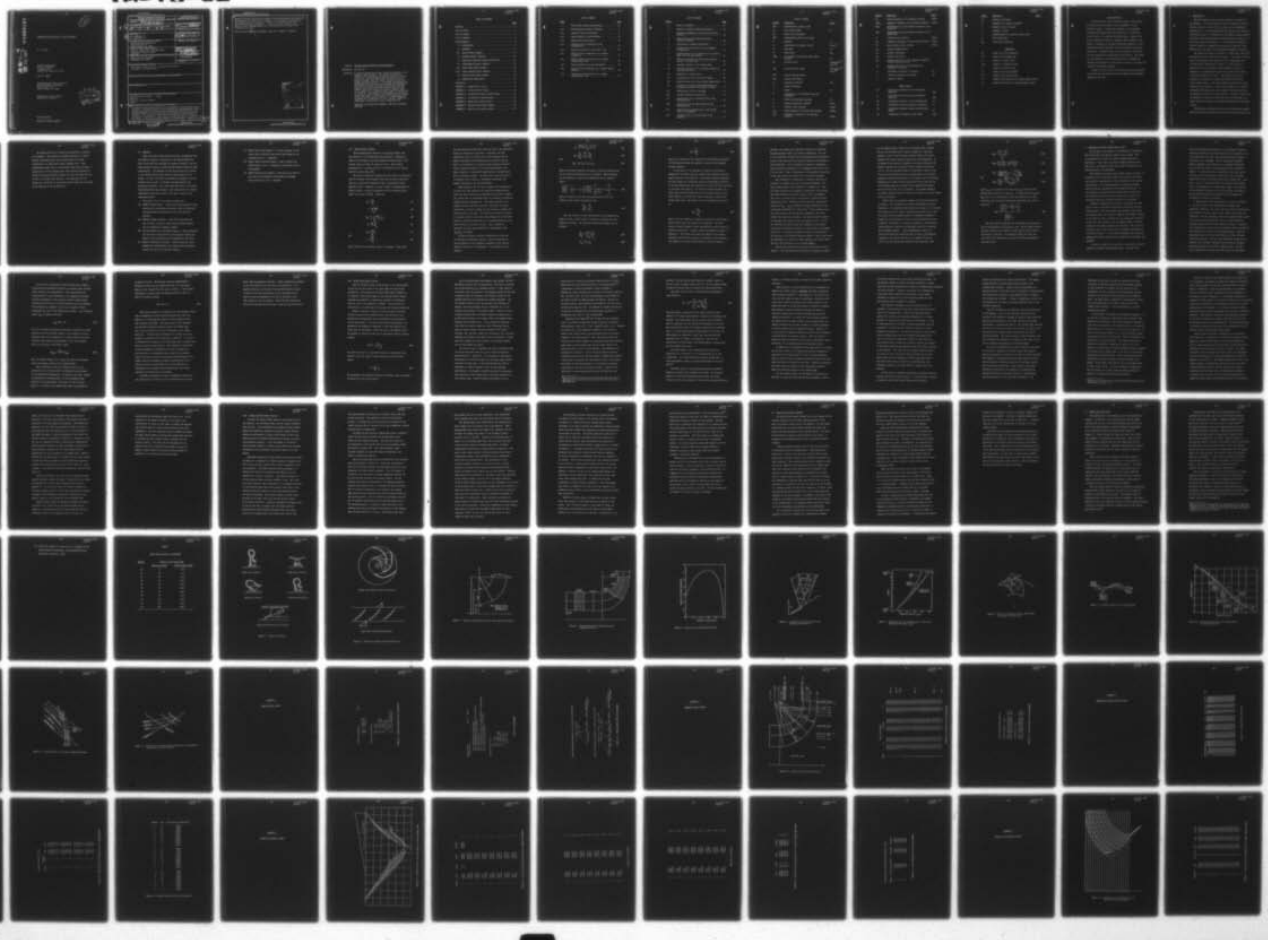

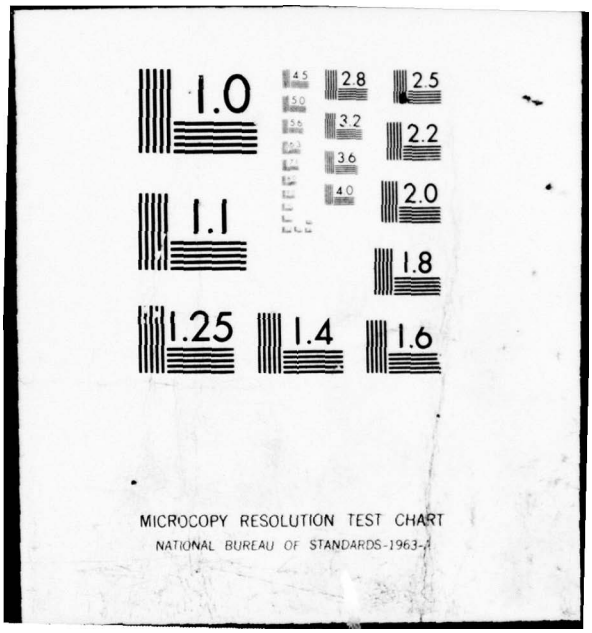
1.0
1.1
1.25
1.4
1.6
1.8
2.0
2.2
2.5
2.8
3.2
3.6
4.0
4.5
5.0
5.6
MICROCOPY RESOLUTION TEST CHART
NATIONAL BUREAU OF STANDARDS-1963-A

12
B.S.

COMPUTER-ASSISTED DESIGN OF PUMP IMPELLERS

M. C. Brophy

Technical Memorandum
File No. TM 78-02
5 January 1978
Contract No. N00017-73-C-1418

Copy No. 57

The Pennsylvania State University
APPLIED RESEARCH LABORATORY
Post Office Box 30
State College, PA 16801

Approved for Public Release
Distribution Unlimited

NAVY DEPARTMENT

NAVAL SEA SYSTEMS COMMAND

UNCLASSIFIED

SECURITY CLASSIFICATION OF THIS PAGE (When Data Entered)

REPORT DOCUMENTATION PAGE

READ INSTRUCTIONS BEFORE COMPLETING FORM

1. REPORT NUMBER ~~TM78-02~~ (14) TM-78-02 | 2. GOVT ACCESSION NO. | 3. RECIPIENT'S CATALOG NUMBER

4. TITLE (and Subtitle) (6)
COMPUTER-ASSISTED DESIGN OF PUMP IMPELLERS

5. TYPE OF REPORT & PERIOD COVERED (9)
Technical memo

6. PERFORMING ORG. REPORT NUMBER

7. AUTHOR(s) (10)
M. C. Brophy

8. CONTRACT OR GRANT NUMBER(s) (15)
N00017-73-C-1418

9. PERFORMING ORGANIZATION NAME AND ADDRESS
Applied Research Laboratory
Post Office Box 30
State College, PA 16801

10. PROGRAM ELEMENT, PROJECT, TASK AREA & WORK UNIT NUMBERS

11. CONTROLLING OFFICE NAME AND ADDRESS
David W. Taylor Naval Ship R&D Center
Annapolis, Maryland 21402
Code 2721

12. REPORT DATE (11)
5 Jan 78

13. NUMBER OF PAGES (12)
~~97~~ 100 p.

14. MONITORING AGENCY NAME & ADDRESS (if different from Controlling Office)
Naval Sea Systems Command
Washington, DC 20362

15. SECURITY CLASS. (of this report)
UNCLASSIFIED

15a. DECLASSIFICATION/DOWNGRADING SCHEDULE

16. DISTRIBUTION STATEMENT (of this Report)
Approved for public release. Distribution unlimited.
Per NAVSEA - 17 January 1978

17. DISTRIBUTION STATEMENT (of the abstract entered in Block 20, if different from Report)

18. SUPPLEMENTARY NOTES

19. KEY WORDS (Continue on reverse side if necessary and identify by block number)
computer-assisted design
impellers
streamline curvature method
blades
pumps

20. ABSTRACT (Continue on reverse side if necessary and identify by block number)
A computer program was written to aid the engineer in the design of pump impellers. The design process first considers the one-dimensional analysis and then proceeds to the two- and three-dimensional construction of the impeller blading that will enable the pump to meet the design operating condition. The program incorporates the Streamline Curvature Method to determine the axisymmetric flow through the pump and employs techniques which are similar to the Mean Streamline Method of blade design. Computer →

DD FORM 1 JAN 73 1473 EDITION OF 1 NOV 65 IS OBSOLETE

391007

UNCLASSIFIED

SECURITY CLASSIFICATION OF THIS PAGE (When Data Entered)

generated plots of the various impeller views are included, and a completed design ready for fabrication is produced. The designer is encouraged at many points within the program to modify the design method as required by his individual needs or desires. A sample design is presented for a pump which is to be used as a model for a high-speed, marine surface craft, propulsion unit.

This work was sponsored by DTNSRDC, Code 2721, Annapolis, Maryland.

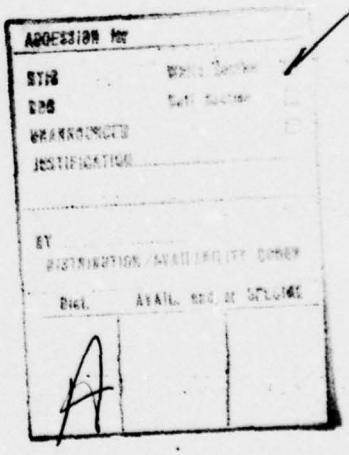

Subject: Computer-Assisted Design of Pump Impellers

References: See page 54.

Abstract: A computer program was written to aid the engineer in the design of pump impellers. The design process first considers the one-dimensional analysis and then proceeds to the two- and three-dimensional construction of the impeller blading that will enable the pump to meet the design operating condition. The program incorporates the Streamline Curvature Method to determine the axisymmetric flow through the pump and employs techniques which are similar to the Mean Streamline Method of blade design. Computer generated plots of the various impeller views are included, and a completed design ready for fabrication is produced. The designer is encouraged at many points within the program to modify the design method as required by his individual needs or desires. A sample design is presented for a pump which is to be used as a model for a high-speed, marine surface craft, propulsion unit.

This work was sponsored by DTNSRDC, Code 2721, Annapolis, Maryland.

TABLE OF CONTENTS

LIST OF TABLES

LIST OF FIGURES

LIST OF SYMBOLS

Symbol	Definition	Units
ADJ	nondimensional advance ratio	
b_2	exit station width	ft
C_L	ideal lift coefficient	
CMS	nondimensional mass rate of flow	
D	diameter	ft
g	acceleration of gravity, 32.174	ft/sec^2
H	pump head	ft
N	shaft speed	rpm
NPSH	net positive suction head above vapor pressure	ft
NS	specific speed	$(rpm)(gpm)^{1/2}/(ft)^{-3/4}$
NSS	suction specific speed	$(rpm)(gpm)^{1/2}/(ft)^{-3/4}$
PBL	percent blockage factor	
PSL	percent slip factor	
Q	volumetric flowrate	cfs
R	radial coordinate	
r	radius	in
S	coordinate for the distance along the streamline	
t	blade circumferential spacing	in
U	impeller tangential velocity	ft/sec
V	absolute fluid velocity	ft/sec
V_{ax}	axial component of the absolute velocity	ft/sec
V_m	meridional component of the absolute velocity	ft/sec

Symbol	Definition	Units
V_r	radial component of the absolute velocity	ft/sec
V_U, V_θ	tangential component of the absolute velocity	ft/sec
VθR	nondimensional V_θ distribution required at the rotor exit	
VθS	nondimensional V_θ distribution required at the stator exit	
W	relative fluid velocity	ft/sec
W_U	tangential component of the relative velocity	ft/sec
$\overline{W}$	mean relative fluid velocity	ft/sec
X_L	percent leakage factor	
X_P	percent prerotation	
X_S	percent slip factor	
X_U	percent reduction in the tangential component of the relative velocity	
X_V	percent reduction in the meridional or through-flow velocity	
x	horizontal coordinate or abscissa	in
y	vertical coordinate or ordinate	in
z	number of blades	

GREEK SYMBOLS

β^*	blade angle measured from the tangential direction	deg
β	fluid angle measured from the tangential direction	deg
Δℓ	incremental distance on the conformal grid	in
Δs	incremental distance along the streamline	in
Δx	incremental distance between conformal grid lines	in
Δθ	incremental arc between radial planes	deg

Symbol	Definition	Units
η_H	hydraulic efficiency	
θ	tangential or angular coordinate	
λ	impeller hub-to-tip ratio	
π	constant, 3.1416	
τ	nondimensional net positive suction head	
ϕ	flow coefficient	
ψ_2	rotor head coefficient	

SUBSCRIPTS

H	value at the hub streamline
LE	value at the leading edge
R	refers to a rotor value
ref	refers to a reference value
S	refers to a stator value
T	value at the tip streamline
TE	value at the trailing edge
1	refers to the entrance (or leading edge) station
2	refers to the exit (or trailing edge) station

ACKNOWLEDGMENTS

The author would like to thank the David W. Taylor Naval Ship Research and Development Center (DTNSRDC) for their financial support. Through their funding, it was possible to attend The Pennsylvania State University on a full-time basis as part of a long-term training program. Appreciation is also extended to Walter S. Gearhart, Mark W. McBride, and Robert E. Henderson of the Applied Research Laboratory at The Pennsylvania State University for their technical assistance and advice. A special thanks is due to George F. Wislicenus for this interest and consultation in this matter. The author is also indebted to the Gas Turbines Branch at DTNSRDC for allowing the completion of this project as part of the water jet propulsion development program.

Support for this effort at the Applied Research Laboratory was provided by the Naval Sea Systems Command through DTNSRDC, Annapolis, Code 2721.

I. INTRODUCTION

The most important aspect of pump design is the design of the impeller. It is this component that will determine how well the pump performs, whether or not it will meet the conditions required of it. In the design problem the desired flow condition is specified, and it is required that the impeller blading provide the proper fluid turning without absorbing excessive power due to fluid losses within the blade row. It is therefore imperative that the impeller be designed as accurately as possible, incorporating into the design sound fundamental hydraulic principles.

The three basic types of impellers -- radial flow, axial flow, and mixed flow, are illustrated in Figure 1. The blades of purely radial flow impellers are designed by way of tangential arcs. In this method, illustrated in Figure 2, a blade section is described by circular segments which smoothly increase the tangential or circumferential sweep of the blade as the radius is increased from inlet to exit. The blades of axial flow impellers are designed by considering cylindrical sections at a constant radius. Here, blade shapes are laid out for each radial location selected, in much the same manner as a cascade, increasing the angular wrap of the blade as the axial distance is traversed from inlet to exit, Figure 2. In each of these cases the designer is required to work only with two dimensions, the other being held constant or arbitrarily specified for each blade section.

The mixed flow impeller as well as the Francis-type impeller, both of which have predominantly axial inlet and radial exit flow,

do not lend themselves to either of these two methods. They are truly three-dimensional problems in that the blade shapes must change in the axial, radial, and tangential direction. Unconventional axial flow impellers, where the hub radius increases from inlet to exit, are also three-dimensional in nature since the streamlines shift outward as they travel through the blades. A method to handle these complicated three-dimensional design problems is presented in this report.

All pump designs begin by utilizing simple one-dimensional considerations, which specify the required parameters at the pump inlet and exit stations. More sophisticated designs employ two-dimensional considerations to analyze the axisymmetric flow field in an attempt to determine what takes place between the pump inlet and exit. However, the design of many pump impellers, as has been pointed out, is truly a three-dimensional problem, and ways must be developed to consider the real fluid flow. The aim of each of these efforts is to somehow construct impeller blades which will allow the pump to operate as designed.

This report is meant to guide the designer through the design process with the help of the computer. The designer will first consider a one-dimensional approach to pump design and attempt to optimize the pump parameters to satisfy performance and operating requirements. Next, the proper two-dimensional axisymmetric pump geometry is selected for this particular design. Then, in the most important step, the blade shapes in three-dimensional space are designed and constructed.

This process if undertaken with the assistance of a computer program written in the Fortran computer language. The computer is operated in conjunction with a CALCOMP plotter which constructs all of the drawings that are normally done by hand at the drafting table. Because of the speed of the digital computer, a design can be completed, modified, and redrawn several times as required; a task that would take the engineer and draftsman weeks to accomplish.

The method of design used by the computer is that of George F. Wislicenus as outlined in Reference 9. It makes use of a conformal mapping which lays out the streamsurfaces on a rectangular grid. In this way, two-dimensional blade shapes can be constructed which, although distorted in the mapping, are true representations of the blading in three-dimensional space. The output of this method provides for the mechanical construction of the blading by producing blade shapes described by board sections which can be built up layer by layer, spanning the entire impeller channel.

By using the computer, steps which would be unnecessarily time-consuming by hand can be undertaken. In this way, many more data points can be used to ensure a more accurate design. The computer program was directly adapted from the graphical procedure, and several refinements in the original design method were incorporated in its development. The program is capable of employing techniques characteristic of the Mean Streamline Method of blade design[5] which has been used with much success in the design of conventional axial flow machines.

An existing design of a Francis-type impeller is included as an example. This impeller represents one-half of a double-suction centrifugal pump, five of which would be located transversely on a high-speed surface planing craft. This configuration makes use of a wide aspect-ratio inlet to ingest a large portion of the boundary layer flow, thereby reducing the amount of internal diffusion required to slow the fluid velocity to that of the pump inlet velocity. The advantages of this system are a reduction in the wetted system weight and a decrease in the momentum of the incoming flow.

II. OVERVIEW

Since the entire design process has been incorporated into the computer program, a discussion of the design method can then be presented by examining the program in detail. The computer program consists of seven separate modules which are used consecutively. The designer in this way can stop at any point in the design process and go back and make changes in the design. In fact, the first two modules are intended to be run several times in order to optimize the pump geometry and operating conditions. Once these items are fixed, the detailed three-dimensional design begins. Each module plots its results independently and provides data to be used as input to the remaining modules.

The modules used in the computer program are:

(1) DESMOD (Design Module) - which allows optimization of pump operating and performance parameters, sizes the impeller, and determines the velocities at the inlet and exit stations.

(2) GEOMTRY (Geometry Module) - which fixes the inlet and exit stations in space by selecting an optimum geometry for the axisymmetric impeller channel.

(3) SCM (Streamline Curvature Method Module) - which determines the velocities and pressures at each station through the pump for each streamline in the axisymmetric flow field.

(4) STREAM (Streamsurface Module) - which divides the three-dimensional streamsurfaces into shapes which approximate squares for use in the conformal mapping.

(5) BLADE (Blade Shape Module) - the most important of the seven, which constructs the actual blade shapes on the conformal grid (S - θ mapping).

(6) RADIAL (Radial Section Module) - which transfers the blade shapes to an R - Z mapping on the profile view of the impeller.

(7) BOARD (Board Section Module) - which plots the axial or plan view of the impeller illustrating the blading board sections on an R - θ mapping.

III. DESIGN MODULE (DESMOD)

The one-dimensional approach to pump design begins with the selection of the design operating condition. Required as input to the design are certain parameters which pertain to the overall system of which the pump is a part. These system parameters are: the head rise, H; the flowrate, Q; and the net positive suction head, NPSH.

The type of impellers considered in this report are characterized by a change in tip diameter from inlet to exit station and thus are a degree more complicated than a conventional axial impeller design. Therefore in order to help in understanding the design process, a series of parameters will be presented which apply to any type of pump[8]. These are:

$$\phi_1 = \frac{V_{ax}}{U_{T_1}} \quad , \tag{1}$$

$$\tau = \frac{2g\ NPSH}{V_{ax}^2} \quad , \tag{2}$$

$$V_{ax} = \frac{4\ Q}{\pi\ D_{T_1}^2\ (1-\lambda^2)} \quad , \tag{3}$$

$$N = \frac{60\ U_{T_1}}{\pi\ D_{T_1}} \quad , \tag{4}$$

$$\psi_2 = \frac{2g\ H}{U_{T_2}^2} \tag{5}$$

and

$$\lambda = \frac{D_{H_1}}{D_{T_1}} \quad , \tag{6}$$

where the hub-to-tip diameter ratio λ is inputed. Since there

are more unknowns (seven) than equations (five), two additional inputs are required at this point. Typically, the flow coefficient ϕ will be varied, and a sixth equation will be added to determine the nondimensional net positive suction head τ as a function of ϕ, based on some cavitation criteria. Another common selection is to fix the shaft speed of the pump, normally at a convenient speed based on the prime mover and its reduction gearbox. In either case, the inlet station is designed first, based on a cavitation requirement and perhaps optimized on the flow coefficient.

These equations are all that is needed for the design of an axial flow pump impeller; the subscripts designating the inlet and exit stations are disregarded in this case. However, for a mixed flow or centrifugal pump, two stations of different diameter must be accounted for. The normal procedure is to design the inlet station to satisfy a cavitation or system constraint, and then to design the exit station to produce the head required of the pump. The first four equations are used in a manner similar to the axial pump design; but in the fifth equation, the head coefficient ψ_2 is calculated based on a tip blade velocity at the exit station. Thus, a method to determine the exit station diameter or the diameter ratio (D_{T_2}/D_{T_1}) is needed.

A direct procedure outlined in Reference 8 allows one to calculate the diameter ratio if a value is selected for the retardation of the tangential component of the relative velocity (relative to the impeller). The equations are as follows:

$$H = \frac{\eta_H (V_{U_2} U_2 - V_{U_1} U_1)}{g} \quad , \tag{7}$$

$$X_U = \frac{W_{U_2}}{W_{U_1}} = \frac{U_2 - V_{U_2}}{U_1 - V_{U_1}} \quad , \tag{8}$$

and

$$V_{U_1} = X_P V_{ax} = X_P U_1 \phi_1 \quad , \tag{9}$$

where an estimated hydraulic efficiency η_H and an expected value for the percent prerotation X_P are estimated. These equations can be combined to arrive at an expression for the diameter ratio:

$$\left(\frac{D_{T_2}}{D_{T_1}}\right)^2 - \left[X_U (1 - X_P \phi_1)\right] \left(\frac{D_{T_2}}{D_{T_1}}\right) + \left[\frac{g H}{\eta_H U_{T_1}^2} + X_P \phi_1\right] = 0 \quad , \tag{10}$$

where the diameter ratio has been substituted for the tip velocity ratio, since from Equation (4),

$$\frac{U_{T_1}}{D_{T_1}} = \frac{U_{T_2}}{D_{T_2}} \quad . \tag{11}$$

The exit station is also characterized by its dimension b_2, Figure 1; thus, another input is required to complete the one-dimensional design. The equations needed and variables are as follows:

$$\frac{b_2}{D_{T_2}} = \frac{Q (1 + X_L)}{\pi D_{T_2}^2 V_{r_2}} \quad , \tag{12}$$

$$V_{r_2} = X_V V_{ax} \quad , \tag{13}$$

and

$$\phi_2 = \frac{V_{r_2}}{U_{T_2}} \quad , \tag{14}$$

where X_V is inserted as the reduction in the meridional component of the velocity through the impeller, and X_L is the estimated flowrate leakage.

At this point, it is possible to construct the velocity diagrams for the inlet and exit stations and calculate the blade angles required of the impeller. The various velocity components and fluid angles are calculated based on trigonometric relations. It is then assumed that the blade angle at inlet β_1^* will correspond to the inlet flow angle β_1. At the exit station, however, the blade angle and fluid angle will not be the same since the real fluid displays an irrotational effect resulting in what can be called fluid slip. The amount of slip is estimated and inputed as

$$X_S = \frac{V_{U_2}}{V_{U_2}^*} \quad , \tag{15}$$

where a star (*) indicates a quantity for which the fluid angle and the blade angle are assumed to be identical. The exit station velocity diagram is then constructed for both starred and unstarred quantities. A sample output from DESMOD is listed in Appendix A. The inputs and outputs are shown for the design condition, and velocity diagrams are included to help visualize the changes in the flow from the inlet to the exit station.

selected, the program will completely construct and describe the pump geometry without any further information. For case 3, it is possible to employ the required geometrical parameters in such a way that nearly any geometry desired by the designer can be specified. For the designer who wants to investigate several different geometries, it is suggested that cases 1 and 2 be run first. Then, if necessary, he can specify the geometry in any other manner by running case 3 as often as desired.

Each streamline is constructed by using two circular arc sections, or possibly three for the center streamline. The blade leading edge is also defined by a circular arc. Thus, the space occupied by the blading is identified, the trailing edge being defined as the exit station at the tip diameter. (For case 3, variable input, a chamfered or oblique trailing edge may be used.) Fictional entrance and exit stations are located $1/2(r_{T_1} - r_{H_1})$ upstream and $1/2(b_2)$ downstream of the actual pump configuration, respectively. These sections allow for fluid entering the leaving the axisymmetric flow field without the effects of curvature. The inner and outer shrouds are assumed to be axial at inlet and radial at exit. If the two circular arcs which define the streamline do not extend all the way to either the entrance or exit section, the program will do so. The center streamline, however, must be defined all the way to the fictional entrance station. This is the reason for allowing it to consist of three segments, the last of which may be a third circular arc or a linear segment.

The data are generated for typically 30 stations overall, Figure 4. The fictional entrance station is selected as number

8, the leading edge as number 16, the trailing edge as number 26, and the fictional exit station as number 30. The seven stations prior to the fictional entrance station are used to generate the velocity profile expected at the leading edge. If an amount of prerotation is expected, the proper turning of the fluid is imparted by a fictional stator located from stations 3 to 6. For the specified amount of prerotation, which in this case is assumed uniform across the leading edge, the necessary tangential velocity distribution at the stator exit is calculated. Differences in radial location between the stator exit and the rotor leading edge are accounted for by applying the equation for free vortex flow ($r\ V_\theta$ = constant). The angular momentum is thereby conserved since no forces are acting on the fluid between these two stations.

Within each of the various segments of the pump illustrated in Figure 4, the streamlines are further subdivided into equal increments. The impeller blading therefore consists of 11 stations, 10 of which are to be loaded, imparting the turning to the flow. The output from the Geometry Module is included in Appendix B. Along with the coordinates for each of the 30 stations and the 3 nominal streamlines, a listing is provided of the additional values needed as inputs by the SCM Module which are calculated by the GEOMTRY program. These nondimensional values are: (1) an area mass flow coefficient CMS, (2) the V_θ distribution required at the stator exit VθS, (3) an advance ratio ADJ, and (4) the V_θ distribution required at the rotor exit, VθR.

$$CMS = \frac{r_{T_1}^2 - r_{H_1}^2}{r_{ref}^2} \quad , \tag{16}$$

$$V\theta S = \frac{r_{LE}}{r_S} \frac{V_{\theta_{LE}}}{V_{ref}} = \frac{r_{LE}}{r_S} \frac{X_P V_{ax}}{V_{ref}} \quad , \tag{17}$$

$$ADJ = \frac{V(in/sec)}{N(\frac{rev}{sec})\ D(in)} = \frac{12\ V_{ref}}{2\ r_{ref}\ (\frac{N}{60})} \tag{18}$$

and

$$V\theta R = \frac{V_{\theta_{TE}}}{V_{ref}} = \frac{\left[\frac{g\ H}{\eta_H} + V_{\theta_{LE}}\ U_{LE}\right]}{U_{TE}\ V_{ref}} \quad , \tag{19}$$

where r_{ref} is set equal to one inch and V_{ref} is equal to the uniform axial velocity at inlet V_{ax}. An expression for U_{LE} and U_{TE} can be found using Equation (4); and Equation (19), which is derived from the Euler pump equation [Equation (7)], can be rewritten:

$$V\theta R = \frac{\left[\frac{g\ H}{\eta_H\ U_{T_1}^2} + \frac{r_{LE}}{r_{T_1}} X_p \phi_{T_1}\right]}{\left(\frac{r_{TE}}{r_{T_1}}\right) \phi_{T_1}} \quad . \tag{20}$$

The plot shown in Appendix B is the graphical representation of the two-dimensional axisymmetric pump. The fictional entrance and exit stations are included, but the sections which include the stator are omitted. All dimensions given are true; that is, they are not affected by the size of the plot indicated by the scale ratio.

V. STREAMLINE CURVATURE METHOD MODULE (SCM)

At this point, the problem of determining the axisymmetric flow field within the impeller channel can be solved. This is accomplished by using the computer program described in Reference 6. Other than a few small changes needed to output data cards, the program remains intact and is included in the design process as the SCM Module.

The Streamline Curvature Method (SCM) is able to define the streamlines for a meridional surface and calculate the radial and convective accelerations of the fluid based on the streamline geometry. The program performs an iterative procedure which continually approximates the streamline locations. It is considered converged when the maximum shift in any one of the streamlines between consecutive passes is reduced to an acceptable tolerance, normally one-tenth of one percent.

The major consideration required of the designer at this point is how to prescribe the streamwise load along the rotor blade stations. With the leading edge unloaded, there remain ten stations which are required to impart the necessary turning to the fluid in order to produce the V_θ distribution specified at the rotor exit station. For the example design, a uniform increase in the angular momentum was selected. The percent of the total load at each station for the uniformly loaded blades is listed in Table 1. It was later determined that a different loading distribution would be more suitable for centrifugal pump blading[3].

In order to enhance the resistance to cavitation inception blades are normally trailing edge loaded. With the rotor

pressure distribution from Reference 5, reproduced in Figure 5, the static pressure on the blade surface is not required to rise too abruptly over the first few stations where the cavitation resistance is at a minimum. With an integration procedure given in Appendix III of Reference 5, a loading distribution for the data from Figure 5 was calculated and is included in Table 1. It can be seen that the percent of the total load is much lower at first and does not equal that for a uniformly loaded blade until the seventh blade station (number 22). From that point on, it clearly exceeds the uniformly loaded blade; hence, its designation as trailing edge loaded. The selection of the loading distribution will directly affect the velocity and streamline locations calculated by the SCM program and ultimately the shape of the blades.

A sample output from the SCM Module is listed in Appendix C. For each station, the nondimensional meridional and tangential velocities, the static and total pressure coefficients, the streamline location, and the local radius of curvature are calculated. The 31 streamlines used in the example design consist of 11 major streamline locations with two pseudo-streamlines included between each for a more accurate solution. As many as 51 streamlines can be used, but as an example, only 7 streamlines were considered for use in the succeeding modules. These are identified as the 1st, 6th, 11th, 16th, 21st, 26th, and 31st streamline locations. For the three-dimensional design of the blading, only stations 8 through 26 are needed, the required data being obtained in the form of punched cards. The data in the example were obtained after 200 passes of the program

where the accuracy had reached six-hundredths of one percent maximum shift in the streamline locations.

VI. STREAMSURFACE MODULE (STREAM)

The Streamsurface Module (STREAM) begins the three-dimensional design of the impeller blading. Since it is extremely difficult to handle three coordinates at any one time, a method of transformation has been employed[9]. In each view of the impeller, one of the coordinates is fixed such that a two-dimensional representation of the blade shapes can be constructed. The first step in this process is to lay out the conformal grid. The method, originally documented by Prasil,[7] transforms the streamsurface into a plane surface in a manner similar to the Mercator Projection of the earth onto a map. The ordinate of the conformal grid corresponds to the distance along the streamline (the arc length coordinate, S), and the abscissa is the blade wrap (the tangential coordinate, θ). It is the purpose of the Streamsurface Module to locate the horizontal grid lines on the streamsurfaces and determine the vertical position on the grid of each of the blade stations.

At this point, it is necessary to examine several figures in order to understand the three-dimensional nature of the problem. The conformal grid on which the blades are to be constructed is actually an output from the Blade Shape Module, and is therefore included in Appendix E as Figure E-1. It displays the S and θ coordinates for each streamline. The output of the Streamsurface Module is the plot shown in Figure D-1. It is a profile view of the pump which displays the R and Z coordinates for each streamline. If a point can be determined by its location on a given streamline, then the radial and axial coordinates can be found.

As an aid in visualizing the grid construction, Figure 6 illustrates the coordinate system for two radial plane sections which intersect the streamsurface. The conformal grid is constructed for a given increment in the tangential direction $\Delta\theta$ which corresponds to the interval at which radial planes extending from the axis of rotation intersect the streamsurface. This increment is assigned a value of arc length Δx which establishes the size of the square grid pattern. A new reference radius r'_{ref} is defined such that

$$r'_{ref}\ (\Delta\theta) = \Delta x \quad . \tag{21}$$

The law of conformal mapping then applies to locations at radii different than the reference radius. Any increment $\Delta\ell$ on the conformal grid that corresponds to a radius different than the reference radius will be proportional to the true increment size by the inverse of the radius ratio:

$$\Delta\ell_{CONF} + \frac{r'_{ref}}{r}\ \Delta\ell_{TRUE} \quad . \tag{22}$$

Thus, the blade thickness at a radius less than the reference radius will appear larger on the conformal grid.

With a knowledge of how the conformal grid is to be constructed, it is now possible to establish the grid points on the meridional streamsurface. In Figure 6 the first "square" is identified by locating point 1 on the streamline which generates the streamsurface. The center of this "square", point C, is located on the radial plane which corresponds to

an angle of 1/2 $\Delta\theta$. The distance along the STREAMLINES is divided such that the arc length from point 0 to the center equals the arc length from the center to point 1. This section approximates a square since the distance from its center to each of its sides is equal,

$$1/2\ r\ \Delta\theta = \Delta s \quad . \tag{23}$$

Since each streamline was defined by the SCM program, points can be established for each horizontal grid line, lines 1-6 Figure E-1, by locating the centers of these "squares" such that Equation (23) holds. The result here is that "squares" are identified which get smaller towards the leading edge, since the arc length for a given $\Delta\theta$ decreases as the radius decreases. (The left side of Figure D-1 is a plot of the arc length as a function of the radius for a given $\Delta\theta$. It is used to determine the location of the grid points and is included here only as an aid in construction.) The locations of grid points on each streamline are indicated by circles on Figure D-1. The locations on the conformal map of each of the stations within the pump are found by calculating the percentage of arc length along the streamlines between horizontal grid lines. These grid lines on the profile view of the impeller are represented by the dashed lines in Figure D-1; the crosses indicate the locations of the stations.

Included in Appendix D is the x-y coordinate location of the intersection of several of the streamlines with the grid

lines (the streamsurface sections). These coordinates correspond to the axial depth Z and the radius R, respectively. In a separate listing, the location of each blade station is given in terms of its vertical position on the conformal grid, a value of zero corresponding to the top of the grid or the exit station at the tip diameter. These data are obtained in the form of punched cards and used as input for the next module.

VII. BLADE SHAPE MODULE (BLADE)

Once the conformal grid is constructed, it is then possible to lay out the exact form of the blade shape for each of the streamlines. The purpose of the Blade Shape Module (BLADE) is to construct these blade shapes on the conformal grid, thereby reducing the problem to a geometrical transfer of coordinates from one view of the impeller to another. The first step in this process is to determine the location of the blade centerline.

Before a decision is made as to how the blade centerline should be placed on the conformal grid, the location of the predicted mean streamline can be determined by the calculation of the blade angles. For each station within the impeller, the meridional and tangential components of the fluid velocity are known from the SCM Module. Referring back to the DESMOD output in Appendix A, the blade angle can be determined from the velocity diagram,

$$\tan \beta^* = \frac{V_m}{U - V_\theta^*} \quad . \tag{24}$$

The blade velocity U at each blade station is calculated using Equation (11); the radial location being known from the SCM output,

$$U = \frac{r}{r_{T_1}} U_{T_1} \quad . \tag{25}$$

The meridional and tangential velocities, however, must be modified to account for real fluid effects.

Due to blade blockage and boundary layer growth, the bulk meridional velocity will be accelerated. This can be accounted for by multiplying V_m by a blockage factor, 1 + PBL, which at this point, must be estimated. The example program was run with a uniform amount of blockage at each station except for the leading edge where the blockage was assumed negligible. For the leading stations, where the boundary layer blockage is minimal, the blade blockage will be significant due to the reduced blade spacing at the smaller radii. However, for the trailing stations where the blade blockage is reduced due to greater blade spacing at the larger radii, the boundary layer blockage becomes significant. It can readily be estimated that these two effects combine to yield a blockage factor which is nearly constant the entire length of the blade.[2] Actually, once the blade shapes are constructed, the true blade blockage and boundary layer growth can be calculated. At that point the designer may want to modify his blockage estimate and run this module over again.

The value for V_θ^* in Equation (24) will be different from the fluid tangential velocity V_θ due to real fluid slip as mentioned before. Therefore, it is necessary to approximate the deviation of the fluid angle from the blade angle towards the blade trailing edge. A slip distribution must then be estimated in a manner similar to that for the blockage distribution. The program currently increases the percentage slip from zero at the leading edge to the value specified at the trailing edge. Another possible distribution for the

slip would be to increase V_θ linearly from the fourth or fifth blade station to the value specified at the trailing edge.[3,9] A comparison of these two methods is shown in Figure 7. Perhaps the linear variation for the slip is a bit more realistic; but, in either case, the real fluid phenomena or the extent of its effect within the blade passage are unknown. However, at the exit station a good estimate can be made for the slip factor as defined by Equation (15). The methods of Stodola and Busemann as outlined in Reference 8 have proven highly successful in determining this factor at the trailing edge.

Wislicenus has suggested[9] that a value for the estimated slip at the blade trailing edge should be within five percent when assuming a value for $1 - PSL = (V_\theta/V_\theta^*)$ equal to 0.8. However, he defines V_θ^* as the tangential component of the velocity based on the relative flow, cross-sectional area of the blade channel at the trailing edge.[8] Thus, the angle at which the fluid exits the blade channel is an average between the specified blade angle at the trailing edge and the larger angle of the adjacent blade at the exit cross-section. This difference is illustrated in Figure 8. Since this cross-section cannot be determined exactly until the blade shape is completely designed,[+] a value must be estimated for the velocity ratio at this point. The effect of this approximation is to increase the required blade angle at exit by a few degrees; hence, a value for the slip ratio a few percentage points below 0.8 should be used

[+]This procedure is based on the Stodola correction and ways to estimate this cross-sectional area, and thus the velocities, are available.

instead. (As can be seen from Figure A-1, smaller values of X_S will result in larger values of β_2^*.) For the example design, a value of 0.78 was used to calculate the slip distribution.

The final equation used to calculate the blade angle at each station is

$$\beta^* = \tan^{-1}\left[\frac{(1 + PBL)\, V_m}{U - \frac{V_\theta}{(1 - PSL)}}\right] . \qquad (26)$$

The blade angles calculated in this manner will most often exhibit an "S" shape characteristic, typical of centrifugal pump blading. The blade angles tend to increase near the leading edge to compensate for the initial blade blockage of the flow, and then decrease slowly to the angle required at the trailing edge. As a precaution against irregularities in the data, the blade angles are smoothed in such a way that distributions exceeding cubic in nature are eliminated. That is, the distribution of blade angles from leading edge to trailing edge may only change slope twice.

The blade angles at the trailing edge can remain as calculated, or, if desired, can be averaged over all of the streamlines. For a pump design with strictly radial exit, it seems reasonable to apply a constant blade angle at the rotor exit.[10]

The blade angles at the leading edge should be modified somewhat to account for incidence of the flow. If the blade angle is in line with the entering fluid angle, the blade is said to be at zero incidence. There may be some justification,

however, to design the blades to operate with a small amount of incidence.

There appears to be some justification for designing the blades with a small amount of negative incidence as measured from the blade centerline.[2] (See Figure 9.) The effort here is to aid the design in terms of cavitation. Cavitation will occur, and a cavity will form on the suction surface of the blade when there is an excessive amount of positive incidence. Even moderate values of positive incidence can result in excessive accelerations, thereby increasing the chance of cavitation inception. To assist the flow in being turned by the blade over the suction surface, and to guard against the effects possible with positive incidence, it seems reasonable to apply a small amount of negative incidence. However, in no way should the negative incidence cause the fluid streamline to extend beyond the pressure surface. This can result in excessive drag on the blades and may lead to separation, and/or cavitation, at the leading edge on the pressure surface.

A similar way of accomplishing this same effect is to align the pressure surface of the blade with the mean streamline as calculated by the blade angles.[9] This in effect guarantees that the flow does not go beyond the pressure surface and still helps the flow to be turned by the blade. Further investigation into this matter may lead to a more satisfactory method to handle the incidence problem at the leading edge.

For the example design, the centerline of the blade was selected to align with the predicted mean streamline; that is,

no further modifications to the blade centerline were made. It is possible, though, to offset the blade centerline or camber line from the mean streamline as is typical of blade design procedures for axial machines.[5] However, since there is no precedent as to how much offset should be incorporated, it was thought sufficient at this point to allow the blade camber line and the predicted mean streamline to coincide.

The effects of blockage, slip, and incidence were all included in the calculation required to place the blade centerline on the conformal grid. Since fluid and blade angles appear true on this type of mapping (conformal), it is then possible to calculate the blade wrap at each station. To aid in understanding this procedure a sample blade shape (the hub streamline) is constructed in Figure 10, identical to that appearing in Figure E-1. The vertical location of each station from the STREAM output and the calculated blade angles were used to calculate the horizontal location of each station on the conformal grid. Except for stations 2 and 10, each segment of the blade centerline was calculated with the station location as its midpoint. The first and last segments (from stations 1 to 2, and 10 to 11) were drawn between stations so that they would align with the leading and trailing edge blade angles. Once the trailing edge is fixed on the conformal map (any convenient location), the blade center or camber line can be plotted.

At this point, a thickness distribution is selected and the pressure and suction surface plotted. A constant blade thickness is normally used, which in many cases may be limited by

foundry considerations for smaller-sized pumps.[9] The example design employed a constant blade thickness equal to the trailing edge thickness. Beyond a point corresponding to a specified amount of the blade chord (for example, fifteen percent), the thickness was allowed to taper linearly until it reached the leading edge thickness. It must be remembered, however, that the thickness to be added to the blade centerline must be the conformal thickness.

The true thickness to be added will thus be distorted due to the mapping. A plot of the thickness distribution as a function of the radius in included in Figure E-1 just above the grid lines and displaced to the right such that zero radius corresponds to vertical grid line D. The trailing edge thickness is true at the reference radius, but decreases for larger radii and increases for smaller radii as required by the law of conformal mapping. The radial location of each streamline will then determine the thickness to be added to each blade station in the conformal representation of the blade shape.

As an aid in determining the radial location of any point on the blade, a mapping of the radius versus the distance along the streamline is plotted on the grid for each streamline. This mapping is constructed using the known radial locations and vertical grid coordinates for each of the blade stations and the horizontal grid lines. Once a point on the blade centerline is identified, the radius can be determined by moving horizontally on the grid, Figure E-1, intersecting the radius mapping for that particular streamline. The

thickness at that point can then be determined by moving vertically on the grid, intersecting the thickness mapping. If this procedure is followed for each station of each streamline, the three surfaces of the blade shape (suction, pressure, and centerline) can be plotted on the conformal grid. The blade shape is completed by constructing a circle for the leading edge with a radius equal to half of the leading edge thickness. It is also possible to use other leading edge shapes.[5]

At this point, the design of the blading is complete. It is now only a problem of transferring these conformal blade shapes just constructed to the proper coordinates required by each view of the impeller. The objective here is to construct board sections[+] on the axial or plan view of the impeller. A plot of this nature, similar to the way in which hull shapes are specified by the naval architect, allows the blading to be fabricated by the pattern maker. This fabrication process described in Reference 1 makes use of boards, cut to the shape of the blade and of a uniform thickness, which correspond to sections passed perpendicular to the axis of rotation and intersecting the blade surface. These can be glued together and smoothed to obtain the exact surface specified by the design. Metal blades could then be cast if the wooden blade is used to make a mold. It is also possible to numerically mill the blades out of metal since the milling machine is capable of cutting the board sections directly.

[+]These will be constructed by the Board Section Module and are illustrated in Figure G-1.

In order to construct the board sections in the axial view of the impeller, the radial and tangential (angular) coordinates (R and θ) are needed for each board section location or axial depth (Z coordinate). From the conformal map, it is possible to obtain both the R and θ coordinates, but no information can be found as to the Z coordinate. It is therefore necessary to transfer the blade shapes to the profile or side view of the impeller, using the R coordinate and the streamline location, for a given radial plane or θ coordinate. In this way, sections of known tangential location can be identified and the R and Z coordinates obtained. These sections, derived from passing planes parallel to the axis of rotation, are labeled radial sections and will be constructed by the next module RADIAL. The Blade Shape Module is therefore required to output all of the coordinate locations needed as input by the Radial Section Module.

Each vertical line (lines A through G) on the conformal grid, Figure E-1, corresponds to a different tangential location. Typically, several lines (which are not shown in Figure E-1) will be passed between vertical grid lines, thereby determining additional radial sections for greater accuracy. The radial coordinate for each tangential location can then be determined, and these coordinates for a sample streamline are included in Appendix E as Table E-1. The trailing edge (which is not a true radial section) is identified by the entry in the last column as radial section number 1, and its centerline is usually positioned such that grid line A is radial section number 2. A problem arises, however, in that the hub streamline blade shape will require more radial sections than the tip streamline

blade shape. A way must therefore be found to handle this leading edge problem.

Because the leading edge is not of itself a streamline, coordinate locations along it are only known at discreet points (i.e., where the leading edge is intersected by the streamlines). Obviously for an infinite number of streamlines, the leading edge would be completely characterized by the streamline stations. However, with only a finite number of these locations known, the leading edge has to be mapped separately in order to transfer it from one view to the next.

For reasons which will become clear in the discussion of the next module, the leading edge was characterized by identifying nine distinct points on each streamline. Thus, the leading edge now consists of nine lines, some of which may not be independent in any one view. Radial sections which would intersect streamlines beyond the leading edge in Figure E-1, can now be seen to intersect these leading edge lines. By identifying the leading edge lines on the profile view of the impeller, incomplete radial sections which do not intersect all of the streamline blade shapes can be completed if the radial coordinate is obtained for the intersection of the radial section with each leading edge line.

In order to find the radial coordinate for the leading edge points, the streamline radius mapping must be used. Leading edge lines can be located on this auxiliary mapping such that the R coordinate for any point on the leading edge line can be found. The R and θ coordinates are listed in Appendix E for one of the nine leading edge points determined

by the incomplete radial sections. The coordinates for each of the leading edge points, identified by crosses on the streamline blade shapes, Figure E-1, will be used to map the leading edge lines in both the profile and the plan view of the impeller.

It is now possible to evaluate the effects of stall or separation on the newly designed blade shapes. The parameter which will be used for this purpose is the lift coefficient. For a known value of the retardation of the relative flow, a limiting value of the lift coefficient can be found from Reference 8. The suggested maximum lift coefficient is illustrated in Figure 11.

The lift coefficient is calculated based on the average relative velocity from inlet to exit.

$$C_L = \frac{2\,(V_{\theta_{TE}}\, t_{TE} - V_{\theta_{LE}}\, t_{LE})}{\bar{W}\, \ell_c} \quad , \tag{27}$$

where

$$t = \frac{2\,\pi\, r}{z} \quad , \tag{28}$$

$$\bar{W} = 1/2\,(W_1 + W_2) \tag{29}$$

and

$$W = [V_m^{\,2} + (U - V_\theta)^2]^{1/2} \quad . \tag{30}$$

If a value is selected for the number of blades z, the lift coefficient for each streamline can be found. The value to be used for the chord length, however, is somewhat deceptive.

(Note that the use of the conformal chord length would be incorrect.) The true chord length is the distance covered by the fluid as it flows along the streamline. For Francis-type impellers, not only does the streamline distance increase in the tangential and axial directions, but it also increases in the radial direction. From the axisymmetric flow field, the distance along the streamline is known (i.e., changes in R and Z), but the tangential distance covered must be approximated. This was done by taking very small increments in length along the streamline, assuming that the chord length could be approximated for each increment as a straight line. Figure 12 illustrates the method used to calculate the true chord length. In this calculation, segments of chord length were equated to straight line segments which connect the two sides of a right triangle -- the distance along the streamline Δs, and the blade wrap $R\,\Delta\theta$.

The lift coefficient was found for each streamline using several different numbers of blades. The values for ten blades are outputed by the Blade Shape Module and are listed in Appendix E. It can be seen that the critical streamline is the tip streamline (number 1) where the chord length is usually a minimum, thus producing a maximum lift coefficient at the smallest value for the retardation of the relative flow.

Based on these values the designer can select the number of blades to be used in the actual pump by making use of Figure 11. Care should be taken in that values for the lift coefficient close to the suggested limit may not be as

conservative as the designer might wish them to be. If the selection of the number of blades at this point is not satisfactory, he could fix the number of blades and redesign the impeller profile to obtain better values for the lift coefficient. The lift coefficient will be reduced for blades of longer chord length by locating the leading edge closer to, or locating the exit station farther (axially) from the entrance station. The value for the retardation of the relative flow will be increased for designs of larger tip diameter and/or smaller exit station width (assuming the parameters at the entrance station are fixed).

VIII. RADIAL SECTION MODULE (RADIAL)

In order to transfer blade shapes to the profile view of the impeller, the streamline number and the radial coordinate must be known. This information was obtained by the previous module and enables the program to construct radial sections (which are determined by a given radial plane) in this view. These sections are plotted identifying the suction, pressure, and centerline surfaces. It is the purpose of the Radial Section Module (RADIAL) to perform this transfer and determine the board section coordinates required as input by the next module.

The BLADE output data can be plotted directly and is shown in Figure F-1 of Appendix F. Radial sections 2 through 26 are seen to span the blade channel from the hub streamline to the tip streamline. The radial sections which correspond to a vertical grid line on the conformal map (Figure E-1) are identified by letters A through G. Also shown in Figure F-1 are the vertical board sections numbered 1 to 19. Up to the 20th radial section, which corresponds to a tangential location on the conformal grid midway between grid lines E and F, the radial sections are complete in that the surfaces intersect all seven streamlines. The pressure surface of these radial sections is the upper solid line and the suction surface is the lower solid line. [From the conformal grid (Figure E-1), it can be seen that a vertical line (or radial section) intersects the suction surface (the lower one) at a point closer to the leading edge of the blade shape, which, from

the radius mapping, corresponds to a smaller radius than that of the centerline. The opposite is true for the pressure surface.] A problem does not arise until the surfaces of the radial sections fail to intersect all of the streamlines, thereby intersecting the leading edge.

By using the nine distinct leading edge points, incomplete radial sections which intersect the leading edge can be drawn with the required accuracy. The only way a point can be identified on this profile view is by its streamline number and radial coordinate (R). Since the incomplete radial sections terminate at locations between streamlines, they cannot be identified directly.

The nine leading edge points are defined from the conformal map and illustrated in Figure 13. Points are identified on each of the suction, pressure, and centerline surfaces at four tangential (or radial plane) locations. The "c" location is calculated to be the point of maximum tangential position and as such can only intersect the pressure surface. The "b" location intersects the centerline at its maximum tangential position and therefore does not intersect the suction surface. The "a" location corresponds to the center of the leading edge circle and also identifies the point of minimum radius on the suction surface. The "z" location is determined such that the "z" pressure surface point is at the same radius as the "b" centerline point. It should be clear that only in the conformal map, where the blade is constructed, is the leading edge actually defined by a circle. This leading edge shape

will change from view to view, depending on the coordinates of the leading edge points for the various types of sections.

The leading edge points identified on the conformal grid can be mapped onto the profile view of the impeller. These leading edge lines, plotted on Figure F-1, represent the area in which the leading edge shapes of the incomplete radial sections are to be plotted. (Because of the reduced scale in Figure F-1, the leading edge lines tend to obscure the shape of the sections within the leading edge area.) A typical leading edge configuration is shown plotted in Figure 14. The grid in this figure consists of blade surfaces intersected by streamlines; however, these streamlines are not necessarily those which are already known. Upon examination of the conformal mapping, Figure E-1, one will find that a radial section (or vertical line) intersects the streamline blade shapes in normally three places, one for each surface. Although these points each correspond to a different radius (as determined by the radius mapping), they are all on the same streamline. If these three leading edge points for each streamline are connected on the conformal grid to form three leading edge lines (samples of which are shown in Figure 13), a radial section which intersects these lines will necessarily define a different streamline by the points of intersection. Thus, vertical sections may be taken through the leading edge which will form streamlines parallel to the known streamlines. Since the R coordinate for each leading edge point was outputed by the Blade Shape Module for each incomplete radial section, the leading edge shapes of these radial sections can be plotted.

At this point, vertical sections can be passed through the radial sections plotted on the profile view of the impeller in Figure E-1. These sections are located using a given increment in the axial direction and identified as board sections, where the blade surfaces are intersected by planes perpendicular to the axis of rotation. The radial and axial coordinates (R and Z) can be found for each board section that intersects a radial section surface. These coordinates are calculated by the program for each radial section; a sample output is included in Appendix F. Coordinates are listed for board sections that intersect each particular radial section surface, beginning at the hub streamline and continuing until the tip streamline is reached. [For the board section plot, the centerline surface is not required.] Board sections which intersect the leading edge lines will be incomplete in the axial or plan view of the impeller. However, because of the leading edge mapping, the coordinates can be obtained for each board section that intersects these leading edge lines. A sample list of these coordinates is also included in Appendix F. Once the leading edge points are mapped on the plan view of the impeller, the incomplete board sections can be constructed using these leading edge coordinates.

Because each blade shape is aligned with the mean streamline, some waviness in the radial sections of Figure F-1 may result. This, in and of itself, is not cause for alarm, but there may be some question as to the shape of these radial sections where they intersect the shrouds. Particularly at the

outer shroud (or tip streamline), it has been pointed out[8,9] that acute angles at this point can result in hydrodynamically unfavorable conditions within the flow passage. The most direct way to alleviate this condition is to properly position the leading edge at the outer shroud as far back as possible, and the leading edge at the inner shroud as close to the entrance as practical. This will result in a leading edge which is closer to a concial surface than a cylindrical surface. To avoid excessively long chord lengths at the hub streamline, the exit blade station should probably be chamfered (creating a blade design which more closely resembles a mixed flow impeller).

Wislicenus has indicated[9] that is may be sufficient to design only the tip streamline blade shape to align with the mean streamline. The tip streamline is the most critical in terms of cavitation, separation, and frictional losses. He suggests that the remaining streamlines be designed and positioned based on primarily geometrical considerations. This will help in lessening the problem of acute angles at the shrouds, but may result in blade shapes that do not impart the proper turning to the flow. Further investigation is needed in this area to guide the designer.

IX. BOARD SECTION MODULE (BOARD)

The Board Section Module (BOARD) is the last segment of the computer program; the only output from this module is the plot of the plan or axial view of the impeller. At this point, practically all of the data points required are known, the majority of them calculated in the previous module. The Board Section Module is therefore only required to plot the R - θ projection of the blading surfaces and to identify the board sections.

A short procedure which was omitted from the last module was incorporated into the BOARD Module. Referring back to Figure F-1, it can be seen that board sections (the vertical lines) which intersect the hub to tip streamlines terminate at these locations. These board sections are not complete in that they do not extend from the leading edge to the trailing edge. Where they intersect either the hub or tip streamline, the surfaces of these board sections are determined by a single point or radial location in Figure F-1. When these end points are transferred to the plan view, they will be seen as an arc, equivalent to the width of the blade at that point, and located at a constant radius from the axis of rotation. At first, board sections will be plotted which start at the trailing edge and terminate on the hub streamline. Depending on the shape of the impeller, a few board sections might extend from the trailing to the leading edges. The remaining board sections will begin at the tip streamline and terminate at the leading edge.

The cylindrical coordinate grid for the plan view of the impeller is laid out in Figure G-1, identifying the radial

planes which appeared as vertical lines on the conformal grid (Figure E-1). The entrance station hub and tip radii are plotted to provide the designer with the view that he would see if he looked directly into the eye of the impeller.

Since the actual blading only extends from the inner shroud to the outer shroud, the hub and tip streamlines will appear in this view as the side boundaries within which the board sections are drawn. Obviously, the leading and trailing edges represent the other two boundaries. The required data for these two streamlines (which are not true board sections, but the locus of the endpoints of an infinite number of board sections) were obtained by the Blade Shape Module from the conformal grid. These streamlines can be plotted and the arcs, where the board sections intersect either the hub or tip streamlines, drawn.

Board sections are drawn in this view of the impeller with the suction surface in the foreground as a solid line and the pressure surface behind it as a dashed line. These surfaces can be plotted directly from the data outputed by the Radial Section Module. Incomplete board sections which intersect the leading edge can be drawn only up to the point where the pressure and suction surface begin to converge.

To aid in constructing the leading edge shapes for each of the incomplete board sections, a mapping of the leading edge lines on the R - θ grid is included in Figure G-1, but displaced a nominal distance in the horizontal direction. A single, solid leading edge line (L.E. point BP) is drawn to connect the hub and tip streamlines. It represents the extreme

surface of the blading as seen by the designer looking into the eye of the impeller. The true or nominal leading edge line (L.E. point BC) is also drawn in Figure G-1 as a dashed line; but, due to the reduced size of the plot, it is not clearly visible.

The data for the incomplete board sections consists of a board section number (or axial coordinate Z) and a radial location (or R coordinate) which corresponds to the point of intersection of the board section with each of the leading edge lines. The θ coordinate can then be determined for each of the nine leading edge points by making use of the leading edge line mapping. In this way, the board section leading edge surfaces are constructed in much the same manner as that used for the incomplete radial sections. Thus, the drawings for the pump impeller design are completed.

X. SUMMARY AND CONCLUSIONS

The fabrication of the blading can now be visualized more clearly. In Figure G-1, each board section, from the large sections near the hub to the small sections near the tip, can be cut from wooden boards of uniform thickness corresponding to the distance between the vertical board sections in Figure F-1. These sections are laid up on top of one another and staggered to approximate the blade shape. They are then glued and later smoothed until the true shape which appears in Figure G-1 is obtained. (Certainly many more board sections than those illustrated could be used to reduce the necessary smoothing.)

Also, since the exact location of the blade surface is known in the plan view of the impeller, it is now possible to evaluate the slip correction approximated earlier. The number of blades defines the spacing at the trailing edge; and, by reproducing this same blade shape at the proper tangential interval, the cross-section at the blade exit can be derived. Either the methods of Stodola and Busemann or Wislicenus, as discussed in Section VII, could then be applied.

The only design quantities from the original one-dimensional analysis which remain unknown at this point are the amount of leakage and the hydraulic efficiency. The leakage cannot be determined until the casing and seals are designed. This would require that the inlet housing as well as the exit housing (normally a volute) be designed, which is a separate part of the overall pump design process.

The hydraulic efficiency is the true measure of the performance of the pump, yet despite this detailed analysis, it must remain only an estimate. Impellers designed in this manner have been built and tested with very good results.[+] The design techniques used by the computer program are based on sound hydrodynamic principles. The hydraulic efficiency has always been determined by experimental testing for any type of pump regardless of its design. However, because of the detailed approach used here, there may be a way to approximate the efficiency in terms of fluid losses. Since the channels within the blade row are defined at many points from the leading edge to the trailing edge, the pertinent velocity and pressure data can be determined. It may then be possible to calculate the frictional, boundary layer, and secondary losses in this manner. Such an efficiency will of course be only an estimate and subject to experimental verification.

Once the designer is satisfied with the pump at its design operating condition, the next step would be to evaluate its off-design performance. Here, it is necessary to determine the actual flow based on the designed blade shapes and a specified inlet condition. Because of the detailed design of the blades, and the thorough characterization of the flow through the impeller, techniques might be derived to solve this, the direct, problem of turbomachinery.

[+] Wislicenus has been responsible for the design of many pumps over the past 40 years. Perhaps the most famous of which is the units installed at the Aswan Colorado State Dam which have demonstrated efficiencies of over 90 percent.

The user of this pump impeller design computer program must, in fact, be the designer or someone working directly under his guiding hand. The program of itself is not a complete design method, but rather a tool to be used by the designer. There are may points along the way which require engineering input and/or evaluation, parts of which may be altered to incorporate or investigate other design techniques. In this way, the designer is able to interact with the computer and produce a detailed hydrodynamic design with which he can be satisfied, in a relatively short amount of time.

The basic advantage of this method is its ability to handle the three-dimensional design problem by making use of the various two-dimensional mappings. The exact procedures programmed are a result of the particular design method selected; however, the pump design would still proceed in much the same manner if another method was used instead. Thus, the designer has not only a tool which can be used to quickly and easily design pump impellers, but also the means to evaluate the design by observing the computer results of the various design changes that could be made.

The goal of the designer is to be able to produce a pump which will meet the requirements specified by the system of which it is a part. This can best be accomplished if the techniques are available to analyze each step of the design process in an attempt to fully understand what is taking place. It is hoped that this pump impeller design computer program is a step in that direction.

REFERENCES

1. Church, Austin H., Centrifugal Pumps and Blowers, Robert E. Krieger Publishing Co., Inc., Huntington, N.Y., 1944.

2. Consultations with W. S. Gearhart at the Applied Research Laboratory, The Pennsylvania State University, September 1976 - May 1977.

3. Conversation with G. F. Wislicenus and M. W. McBride at the Applied Research Laboratory, The Pennsylvania State University, August 1977.

4. Dixon, S. L., Fluid Mechanics, Thermodynamics of Turbomachinery, Pergamon Press, Oxford, England, 1975.

5. McBride, M. W., Computerization of the Mean Streamline Blade Design Method, Applied Research Laboratory, The Pennsylvania State University, TM 73-22, February 1973.

6. McBride, M. W., A Streamline Curvature Method of Analyzing Axisymmetric Axial, Mixed and Radial Flow Turbomachinery, Applied Research Laboratory, The Pennsylvania State University, TM 77-219, July 1977.

7. Prasil, Technische Hydrodynamik, Julius Springer Publishers, 1926.

9. Wislicenus, George F., Fluid Mechanics of Turbomachinery, Dover Publications, N.Y., 1965.

9. Wislicenus, George F., "The Design of Centrifugal Pumps with Special Emphasis on Cavitation," Proceedings of the Fluid Dynamics Institute, Hanover, N.H., Radial Flow Turbomachinery, August 1976.

10. Wislicenus, George F., Letter to W. S. Gearhart at the Applied Research Laboratory, The Pennsylvania State University, February 1, 1977.

TABLE 1

ROTOR BLADE LOADING DISTRIBUTIONS

Station	Percent of the Total Load	
	Uniformly Loaded	Trailing Edge Loaded
16	0	0.0
17	10	6.3
18	20	15.0
19	30	25.2
20	40	36.5
21	50	48.3
22	60	60.5
23	70	72.7
24	80	84.3
25	90	94.5
26	100	100.0

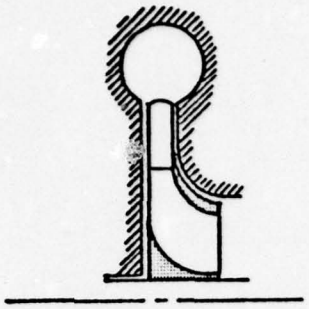

Radial Flow Impeller

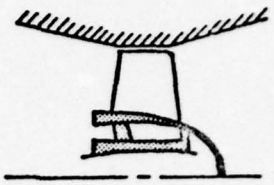

Axial Flow Impeller

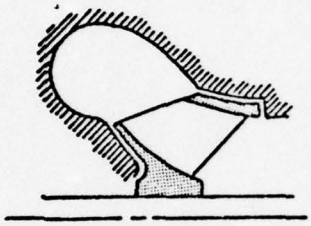

Mixed Flow Impeller

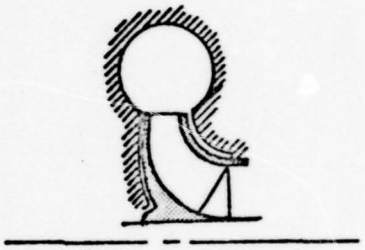

Francis-Type Impeller

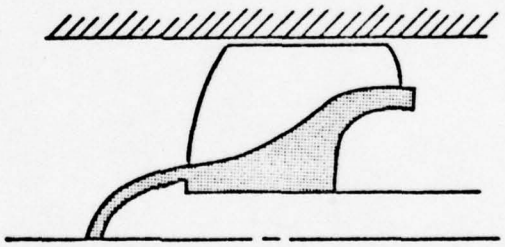

Unconventional Axial Flow Impeller

Figure 1 - Types of Impellers

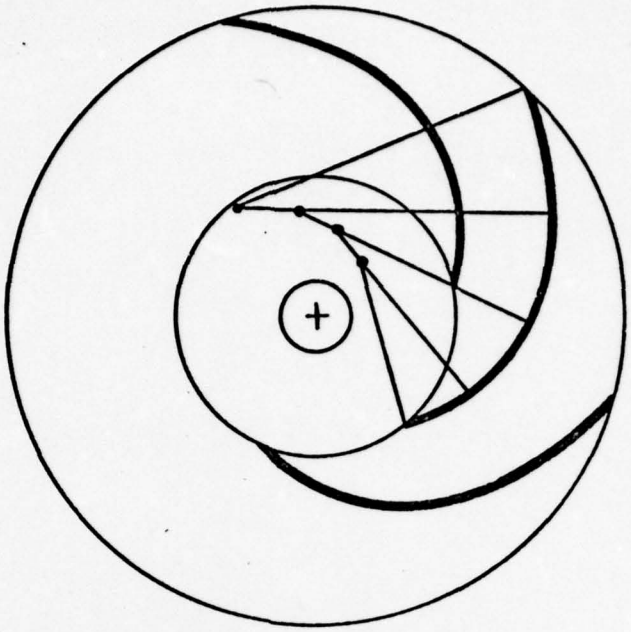

Radial Flow Impeller Blade Construction

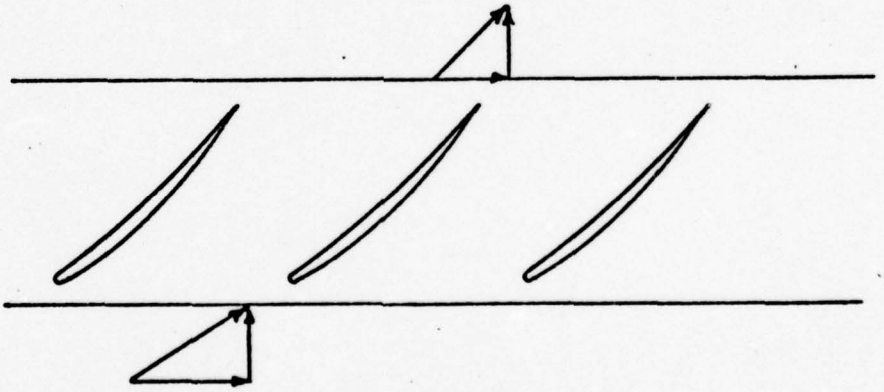

Axial Flow Cascade Representation

Figure 2 - Methods of Impeller Blade Construction

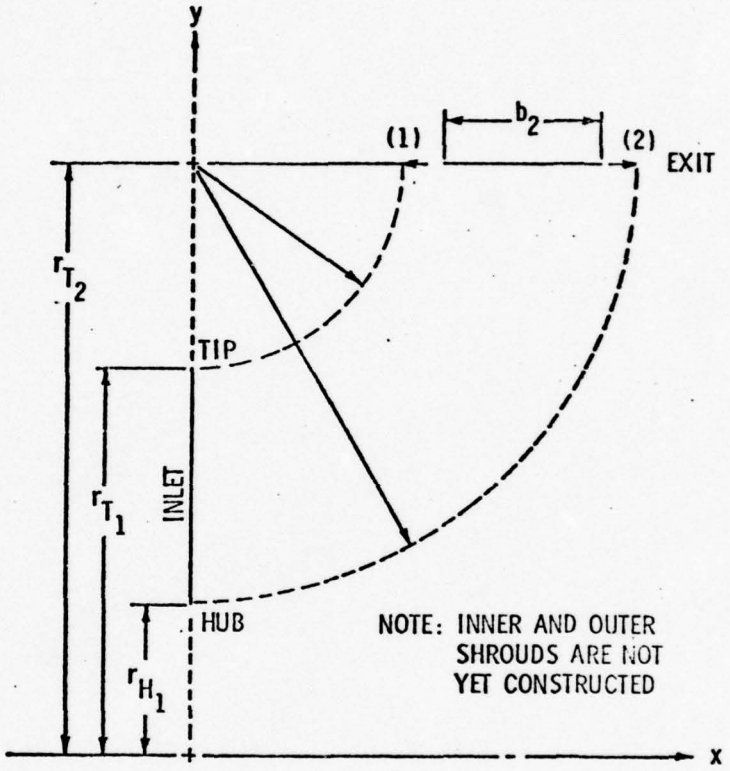

Figure 3 - Relative Configuration of the Inlet and Exit Stations

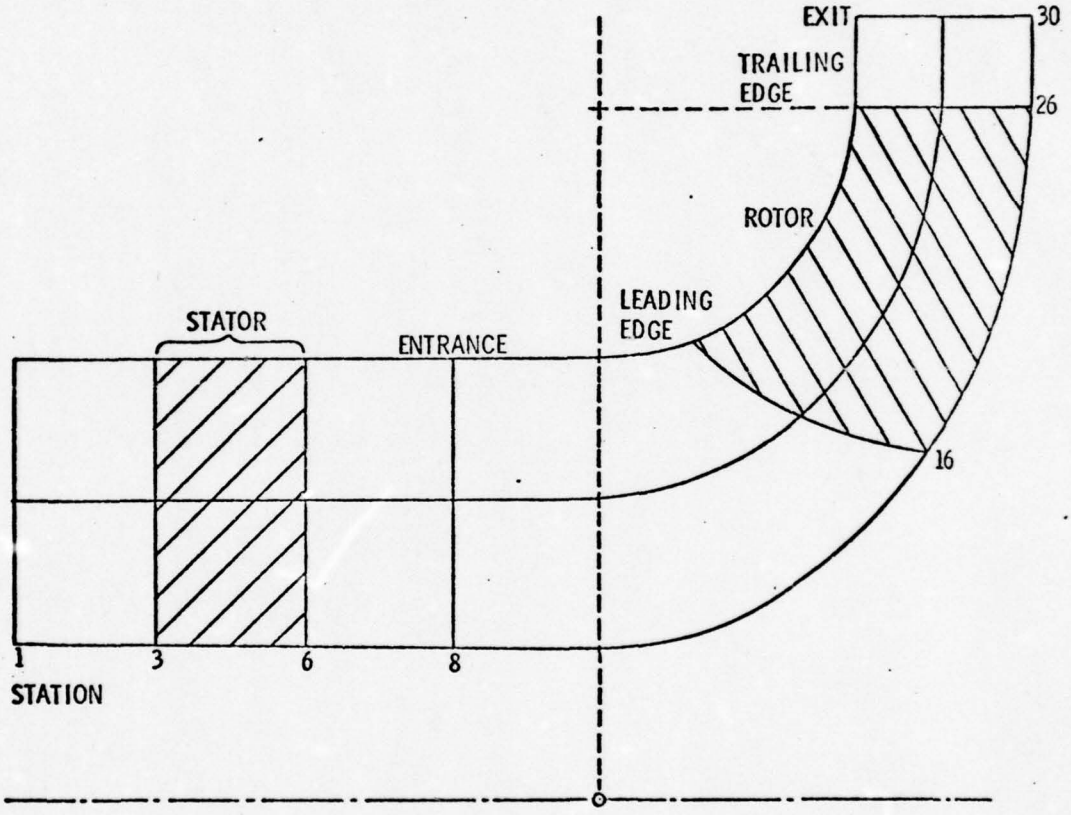

Figure 4 - Pump Configuration Indicating Various Component Stations

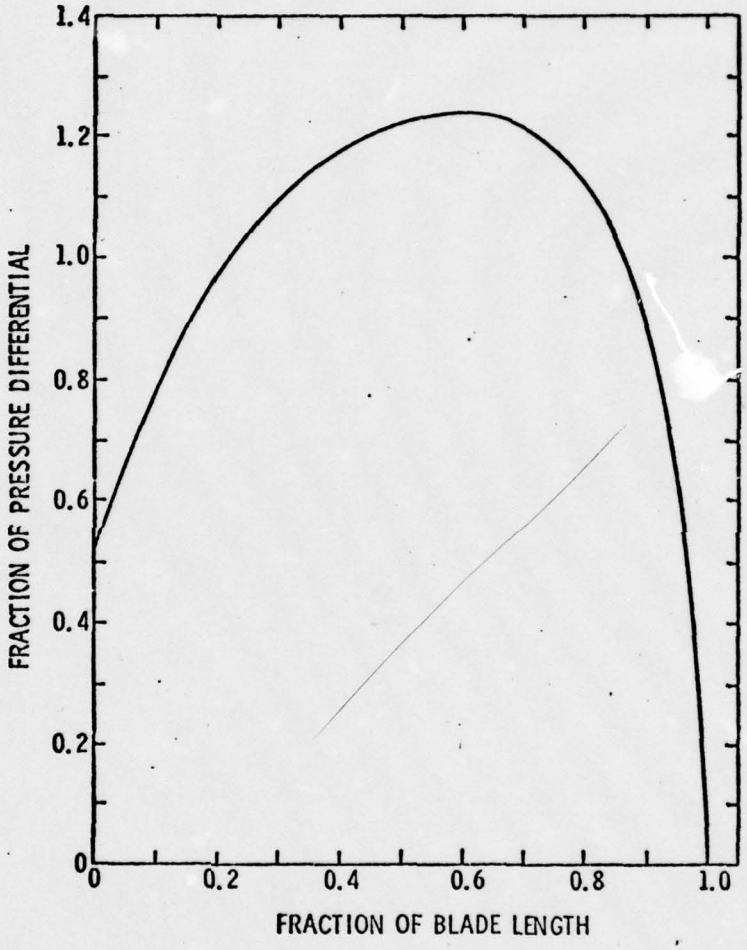

Figure 5 - Typical Rotor Loading Distribution

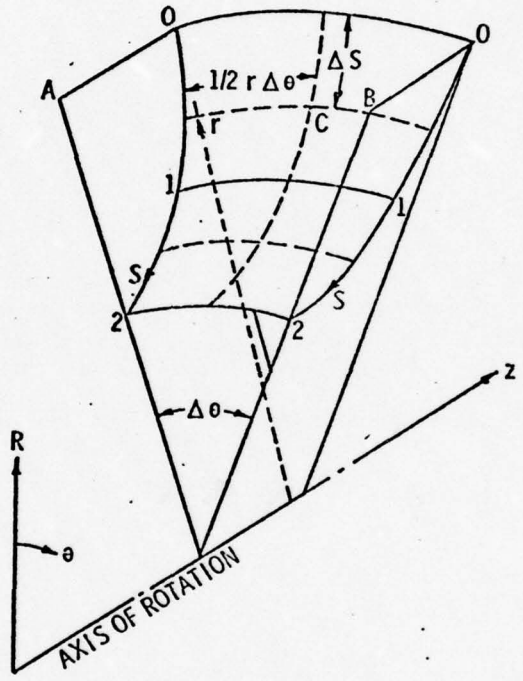

Figure 6 - Construction of Grid Lines on the Impeller Streamsurface

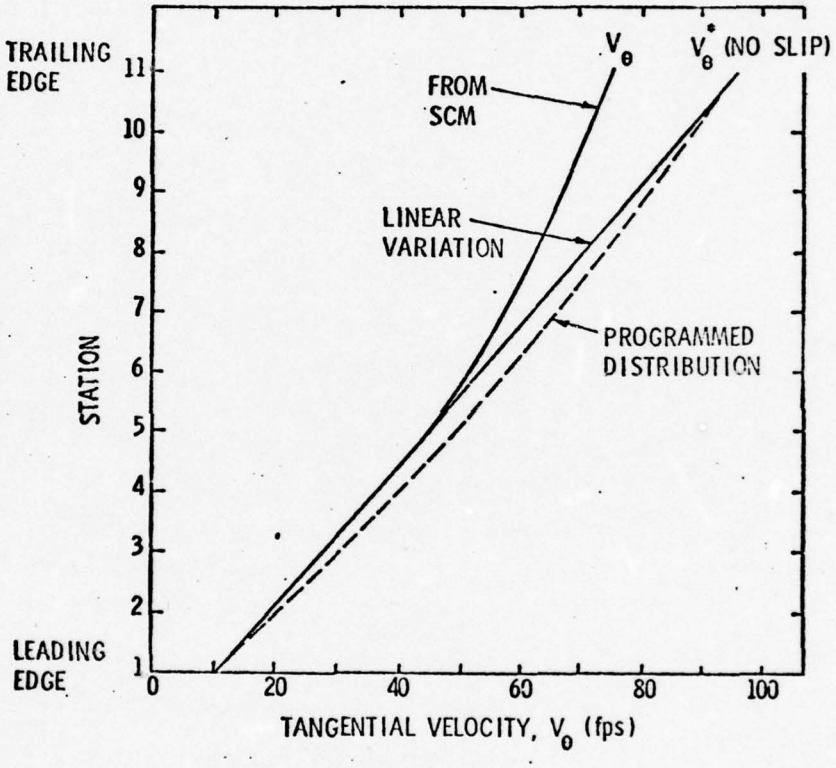

Figure 7 - Approximations for the Deviation of the Fluid Angle from the Blade Angle

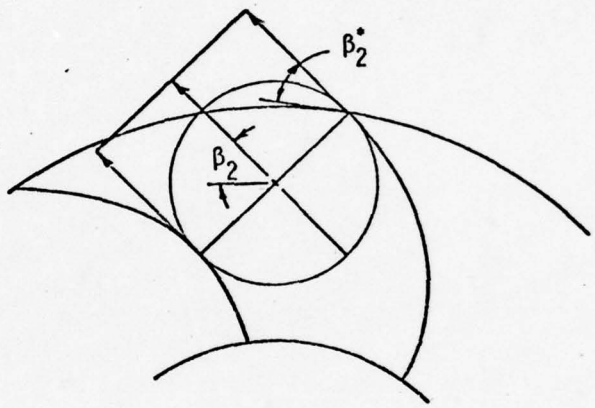

Figure 8 - Method to Determine the Exit Blade Angle to Account for Fluid Slip

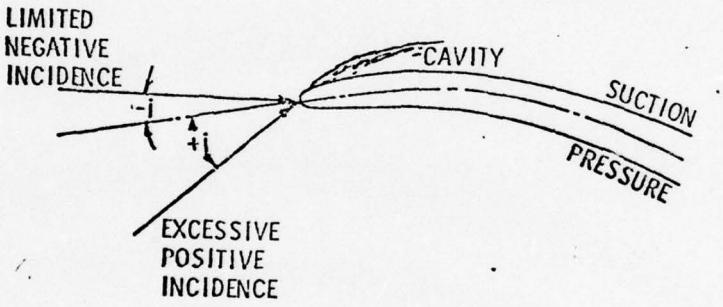

Figure 9 - Incidence Effects at the Leading Edge

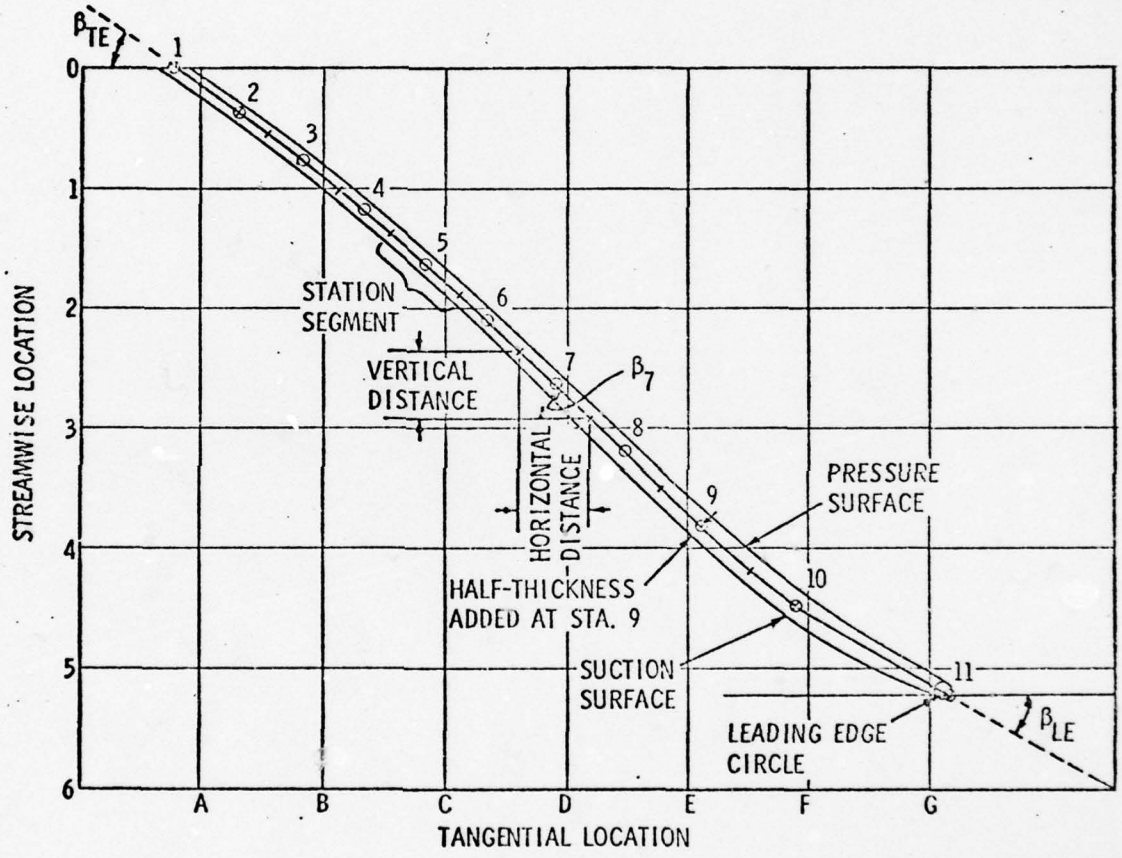

Figure 10 - Detailed Construction of the Blade Shapes on the Conformal Grid

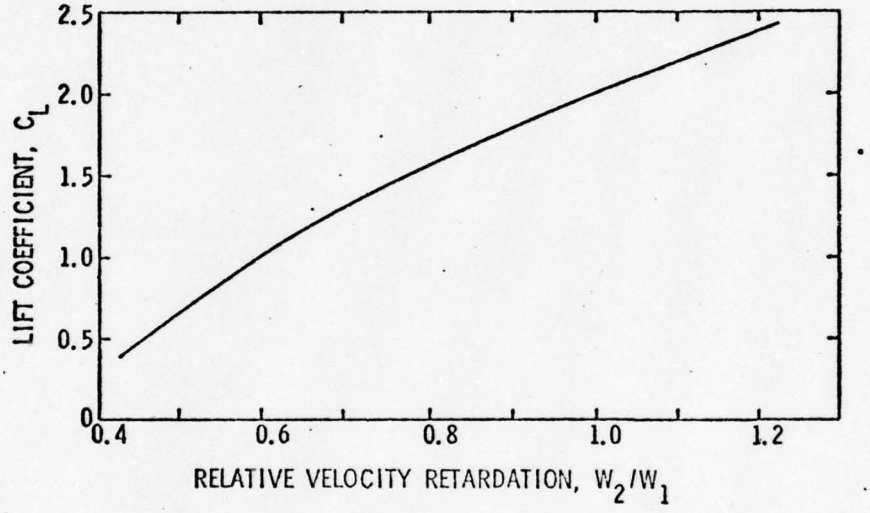

Figure 11 - Separation of Stall Limits

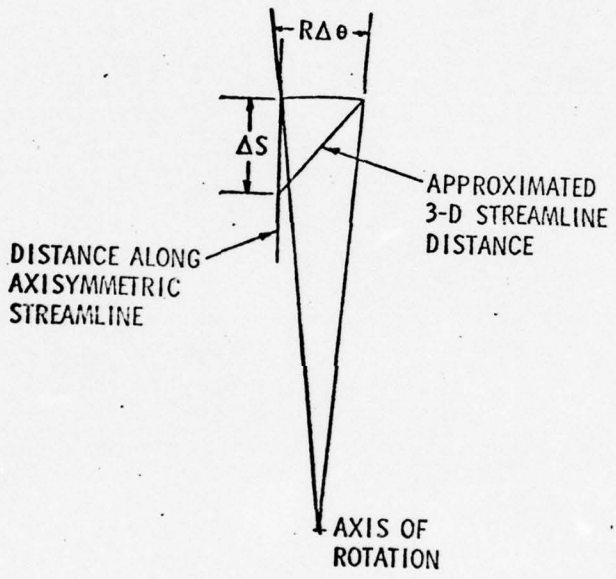

Figure 12 - Determination of the True Chord Length

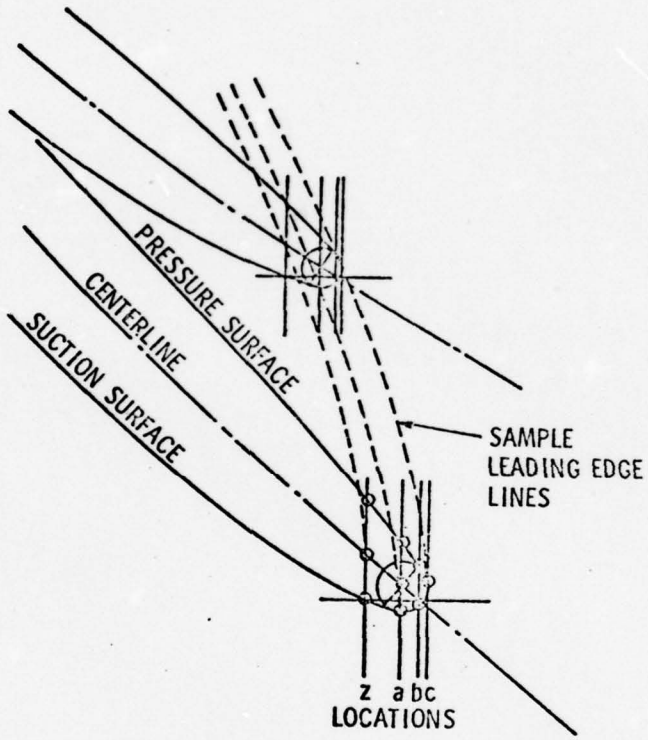

Figure 13 - Identification of the Nine Leading Edge Points

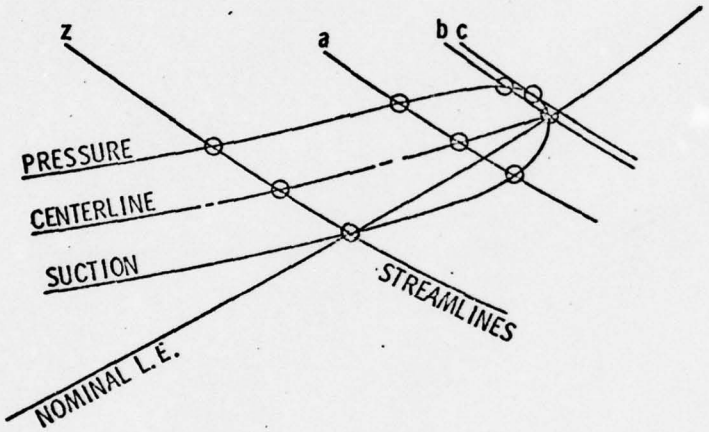

Figure 14 - Location of the Nine Leading Edge Points on Streamlines Determined by Radial Sections

APPENDIX A

DESIGN MODULE OUTPUT

THE SYSTEM DESIGN PARAMETERS ARE RUN NO. 1

HEAD = 291.700 (FT)
FLOWRATE = 13205.00 (GPM)
NPSH = 82.0000 (FT)

THE INLET PUMP DESIGN PARAMETERS ARE

PHI1 = .438980
TAU = 3.10454
VAX = 40.8334 (FT/SEC)
UT1 = 133.3944 (FT/SEC)
DT1 = .948280 (FT)
DH1 = .435209 (FT)
(LAMDA = .469330)
N = 2055.000 (RPM)
NS = 3021.574 (RPM)(GPM)1/2(FT)-3/4
NSS = 7522.00 (RPM)(GPM)1/2(FT)-3/4

Table A-1 - Design Operating Point Parameters

DETAILED PUMP DESIGN RUN NO. 1 TRIAL NO. 1

THE SPECIFIED INPUTS ARE

.980000 PERCENT REDUCTION IN THE RELATIVE VELOCITY

.800000 PERCENT REDUCTION IN THE TANGENTIAL COMPONENT OF THE RELATIVE VELOCITY

.900000 PERCENT RETARDATION OF THE THRU-FLOW VELOCITY

.250000 PERCENT PRE-ROTATION

.220000 ESTIMATED PERCENT SLIP (REDUCTION IN THE TANGENTIAL COMPONENT OF THE ABSOLUTE VELOCITY)

.015000 ESTIMATED PERCENT FLOWRATE LEAKAGE DUE TO PRESSURE SEALS

.890000 ESTIMATED PUMP HYDRAULIC EFFICIENCY

THE OUTLET PUMP DESIGN PARAMETERS ARE

PHI2 = .219641

PST2 = .112319

VR2 = 32.6670 (FT/SEC)

UT2 = 149.4394 (FT/SEC)

DT2 = 1.397890 (FT)

DT2/DT1 = 1.6433971

D2 = .162029 (FT)

D2/DT2 = .1157691

Table A-1 (continued)

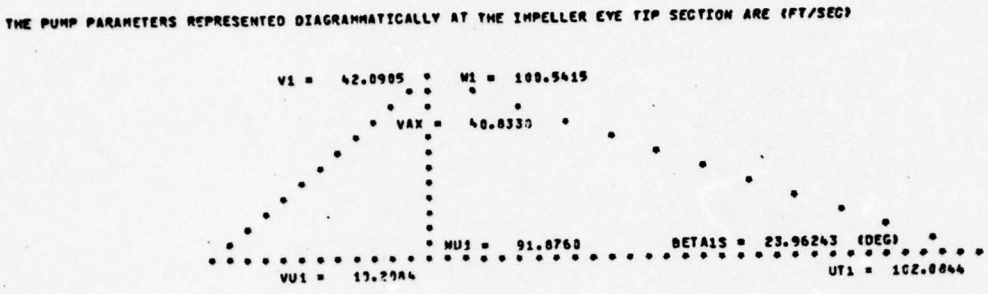

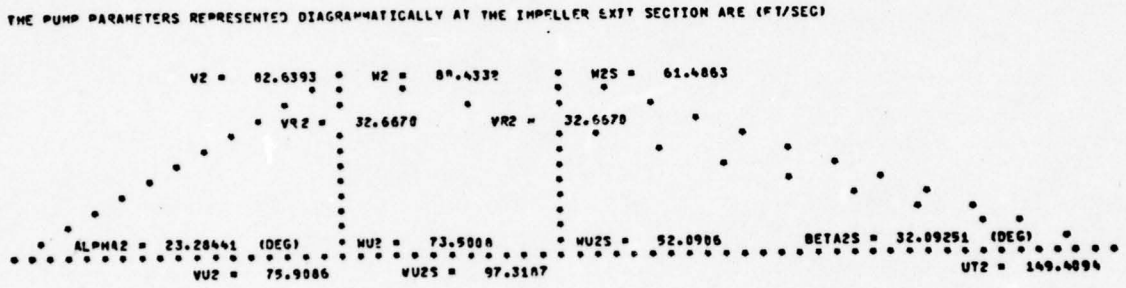

Figure A-1 - Design Module Velocity Diagrams

APPENDIX B

GEOMETRY MODULE OUTPUT

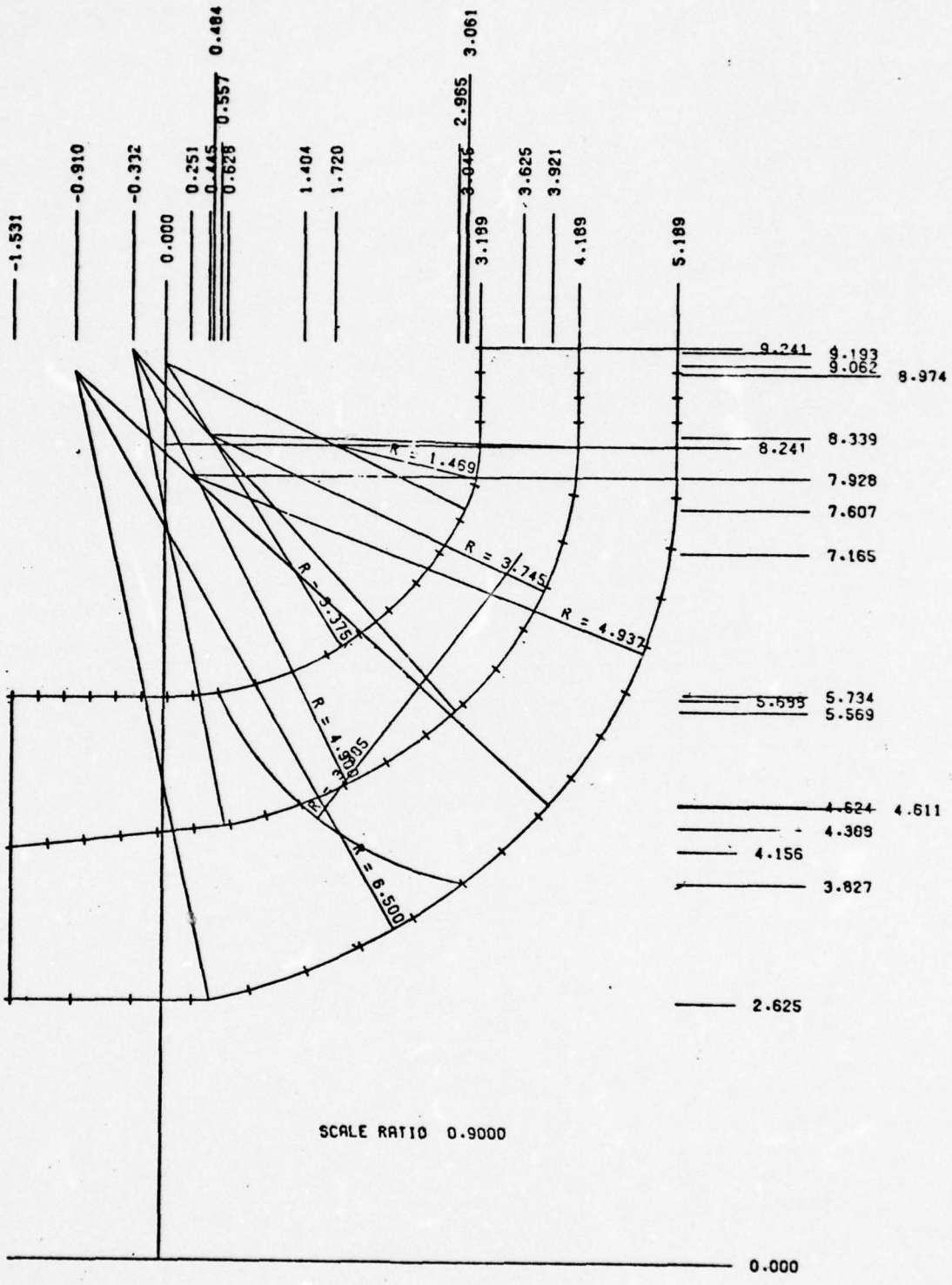

Figure B-1 - Impeller Geometric Construction

IMPELLER STATION COORDINATES

STATION	HUB		CENTERLINE		TIP		
1	-6.125000	2.625000	-6.125000	4.156250	-6.125000	5.687500	
2	-5.359375	2.625000	-5.359375	4.156250	-5.359375	5.687500	
3	-4.593750	2.625000	-4.593750	4.156250	-4.593750	5.687500	STATOR LE
4	-4.083334	2.625000	-4.083334	4.156250	-4.083334	5.687500	
5	-3.572917	2.625000	-3.572917	4.156250	-3.572917	5.687500	
6	-3.062500	2.625000	-3.062500	4.156250	-3.062500	5.687500	STATOR TE
7	-2.296875	2.625000	-2.296875	4.156250	-2.296875	5.687500	
8	-1.531250	2.625000	-1.531250	4.156250	-1.531250	5.687500	ENTRANCE
9	-.921870	2.625000	-1.160925	4.195995	-1.269845	5.687500	
10	-.310791	2.625000	-.790599	4.235740	-1.008441	5.687500	
11	.299439	2.625000	-.420273	4.275485	-.747036	5.687500	
12	.896449	2.729745	-.049948	4.315231	-.485631	5.687500	
13	1.473865	2.926580	.320378	4.354976	-.224227	5.687500	
14	2.030246	3.174673	.689742	4.400759	.037177	5.687705	
15	2.569743	3.477923	1.050700	4.492207	.298194	5.708699	
16	3.060652	3.827376	1.403672	4.610882	.557422	5.733851	ROTOR LE
17	3.452247	4.154828	1.849124	4.885343	.936782	5.020091	
18	3.816938	4.511944	2.273109	5.043862	1.303541	5.949398	
19	4.150079	4.898651	2.671454	5.321519	1.653866	6.120053	
20	4.441977	5.317296	3.040019	5.638513	1.980635	6.329789	
21	4.689191	5.763835	3.367803	5.997258	2.281898	6.575822	
22	4.888410	6.233499	3.646377	6.395411	2.552852	6.854883	
23	5.038971	6.721269	3.871052	6.826298	2.789898	7.163265	
24	5.137979	7.221934	4.038043	7.287633	2.989890	7.496874	
25	5.184777	7.730144	4.144540	7.756757	3.137491	7.856040	
26	5.188750	8.240679	4.188750	8.240679	3.188750	8.240679	ROTOR TE
27	5.188750	8.490679	4.188750	8.490679	3.188750	8.490679	
28	5.188750	8.740679	4.188750	8.740679	3.188750	8.740679	
29	5.188750	8.990679	4.188750	8.990679	3.188750	8.990679	
30	5.188750	9.240679	4.188750	9.240679	3.188750	9.240679	EXIT

Table B-1 - Impeller Station Coordinates

INPUTS FOR THE STREAMLINE CURVATURE PROGRAM ARE

THE MASS FLOW COEFFICIENT = 25.45703

V-THETA AT STATOR EXIT HUB STREAMLINE = .364512
V-THETA AT STATOR EXIT CENTER STREAMLINE = .277341
V-THETA AT STATOR EXIT TIP STREAMLINE = .252037

THE ADVANCE RATIO = 7.143969

V-THETA AT ROTOR EXIT HUB STREAMLINE = 1.023431
V-THETA AT ROTOR EXIT CENTER STREAMLINE = 1.047198
V-THETA AT ROTOR EXIT TIP STREAMLINE = 1.081268

Table B-2 - Inputs Needed by the SCM Module

APPENDIX C

STREAMLINE CURVATURE METHOD OUTPUT

SLC OUTPUT FOR STATION 15

SL	PCT-SPAN	V-MERIDIONAL	V-TANGENTIAL	CP-STATIC	CP-TOTAL	X/R-REF	R/R-REF	R-CURV/R-REF	V-AXIAL
1	0.	.827734E+00	.249998E+00	.252960E+00	.100060E+01	3.0507	3.0291	0.	
2	.4581E-01	.834174E+00	.254449E+00	.240028E+00	.100062E+01	2.8980	3.0718	-.645382E+01	
3	.9330E-01	.840845E+00	.257515E+00	.227299E+00	.100063E+01	2.7493	3.9167	-.619087E+01	
4	.1393E+00	.847981E+00	.259457E+00	.214257E+00	.100055E+01	2.6051	3.9658	-.595132E+01	
5	.1948E+00	.855753E+00	.260531E+00	.200484E+00	.100066E+01	2.4657	4.0182	-.573388E+01	
6	.2295E+00	.864127E+00	.260837E+00	.185925E+00	.100067E+01	2.3312	4.0734	-.553978E+01	
7	.2734E+00	.872992E+00	.260631E+00	.170633E+00	.100068E+01	2.2020	4.1312	-.537167E+01	
8	.3164E+00	.882275E+00	.260026E+00	.154663E+00	.100058E+01	2.0780	4.1912	-.523062E+01	
9	.3585E+00	.891934E+00	.259144E+00	.137991E+00	.100069E+01	1.9593	4.2533	-.511384E+01	
10	.3996E+00	.901954E+00	.258091E+00	.120569E+00	.100070E+01	1.8458	4.3169	-.501605E+01	
11	.4396E+00	.912315E+00	.256958E+00	.102361E+00	.100071E+01	1.7375	4.3819	-.493239E+01	
12	.4785E+00	.922961E+00	.255822E+00	.834091E-01	.100072E+01	1.6342	4.4481	-.485810E+01	
13	.5164E+00	.933851E+00	.254747E+00	.637488E-01	.100072E+01	1.5358	4.5151	-.478862E+01	
14	.5532E+00	.944960E+00	.253787E+00	.433737E-01	.100073E+01	1.4421	4.5828	-.472064E+01	
15	.5888E+00	.956349E+00	.252968E+00	.221435E-01	.100074E+01	1.3535	4.6507	-.465342E+01	
15	.6230E+00	.968434E+00	.252241E+00	-.749968E-03	.100075E+01	1.2712	4.7197	-.458819E+01	
17	.6557E+00	.981272E+00	.251604E+00	-.254419E-01	.100076E+01	1.1951	4.7893	-.452552E+01	
18	.6872E+00	.994800E+00	.251060E+00	-.518906E-01	.100077E+01	1.1247	4.8594	-.446597E+01	
19	.7173E+00	.100897E+01	.250609E+00	-.790541E-01	.100078E+01	1.0594	4.9296	-.440756E+01	
20	.7461E+00	.102375E+01	.250250E+00	-.109991E+00	.100079E+01	.9990	4.9998	-.434951E+01	
21	.7739E+00	.103910E+01	.249976E+00	-.141412E+00	.100080E+01	.9430	5.0697	-.429019E+01	
22	.8005E+00	.105499E+01	.249780E+00	-.174598E+00	.100081E+01	.8910	5.1391	-.422774E+01	
23	.8260E+00	.107144E+01	.249655E+00	-.209505E+00	.100082E+01	.8427	5.2080	-.416017E+01	
24	.8506E+00	.108847E+01	.249593E+00	-.246236E+00	.100083E+01	.7978	5.2763	-.408338E+01	
25	.8743E+00	.110613E+01	.249577E+00	-.284977E+00	.100084E+01	.7560	5.3439	-.399223E+01	
26	.8971E+00	.112453E+01	.249606E+00	-.326014E+00	.100085E+01	.7170	5.4108	-.388598E+01	
27	.9191E+00	.114379E+01	.249665E+00	-.369722E+00	.100086E+01	.6807	5.4769	-.377321E+01	
28	.9403E+00	.116399E+01	.249746E+00	-.416239E+00	.100087E+01	.6468	5.5422	-.367640E+01	
29	.9608E+00	.118486E+01	.249940E+00	-.465411E+00	.100088E+01	.6151	5.6067	-.360004E+01	
30	.9807E+00	.120643E+01	.249930E+00	-.517648E+00	.100089E+01	.5854	5.6706	-.354494E+01	
31	.1000E+01	.122951E+01	.250003E+00	-.570441E+00	.100090E+01	.5574	5.7339	-.350268E+01	

Table C-1 - Sample SCM Station Output

APPENDIX D

STREAMSURFACE MODULE OUTPUT

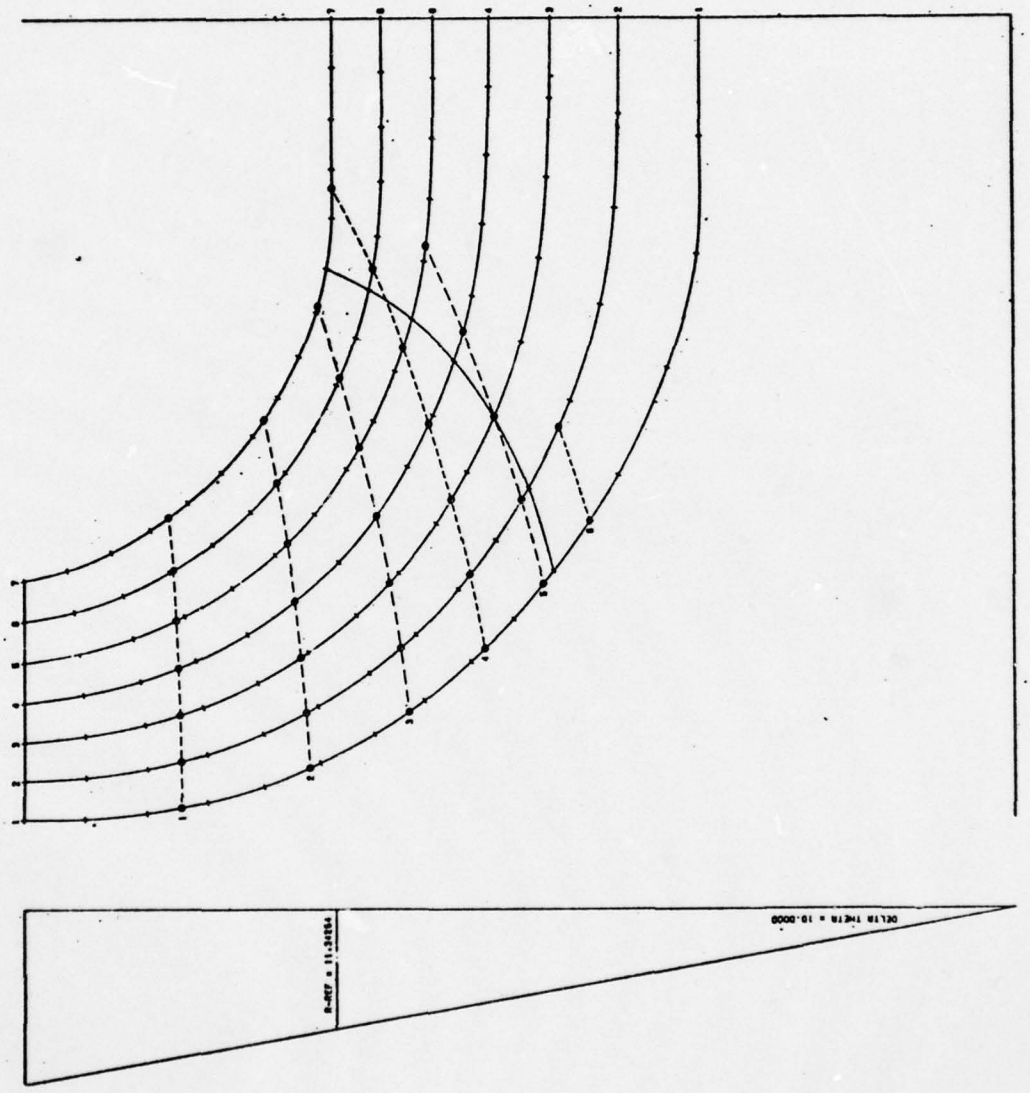

Figure D-1 - Construction of the Conformal Grid on the Streamsurfaces

STREAMSURFACE COORDINATES ARE AS FOLLOWS

STREAMLINE	STREAMSURFACE SECTION	X-COORD	Y-COORD
1	1	-13.1914	13.9141
1	2	-12.5248	11.7826
1	3	-11.5982	10.1216
1	4	-10.5335	8.8519
1	5	-9.4616	7.8691
1	6	-8.4118	7.0927
2	1	-12.4227	13.9264
2	2	-11.6044	11.8420
2	3	-10.5178	10.2578
2	4	-9.3023	9.0954
2	5	-8.0602	8.2381
2	6	-6.8408	7.5952
3	1	-11.6448	13.9462
3	2	-10.6769	11.9195
3	3	-9.4330	10.4388
3	4	-8.0494	9.4042
3	5	-6.6560	8.6776
4	1	-10.8592	13.9724
4	2	-9.7349	12.0184
4	3	-8.3207	10.6541
4	4	-6.7830	9.7687
4	5	-5.2412	9.1887

Table D-1 - Conformal Grid Coordinates on the Streamsurface

5 January 1978
MCB:jep

STREAMLINE	STATION	PERCENT ARC-LENGTH FOR CONFORMAL MAPPING
1	16	0.000000
1	15	.384834
1	14	.779588
1	13	1.195790
1	12	1.636975
1	11	2.102144
1	10	2.638487
1	9	3.198811
1	8	3.818639
1	7	4.478497
1	6	5.281124
2	16	0.000000
2	15	.398369
2	14	.781584
2	13	1.202019
2	12	1.647505
2	11	2.114283
2	10	2.648570
2	9	3.208126
2	8	3.814227
2	7	4.468589
2	6	5.171341
3	16	0.000000
3	15	.387664
3	14	.778456
3	13	1.183537
3	12	1.627787
3	11	2.078053
3	10	2.608771
3	9	3.131743
3	8	3.727053
3	7	4.341484
3	6	4.947154

Table D-2 - Station Locations for Each Streamline

APPENDIX E

BLADE SHAPE MODULE OUTPUT

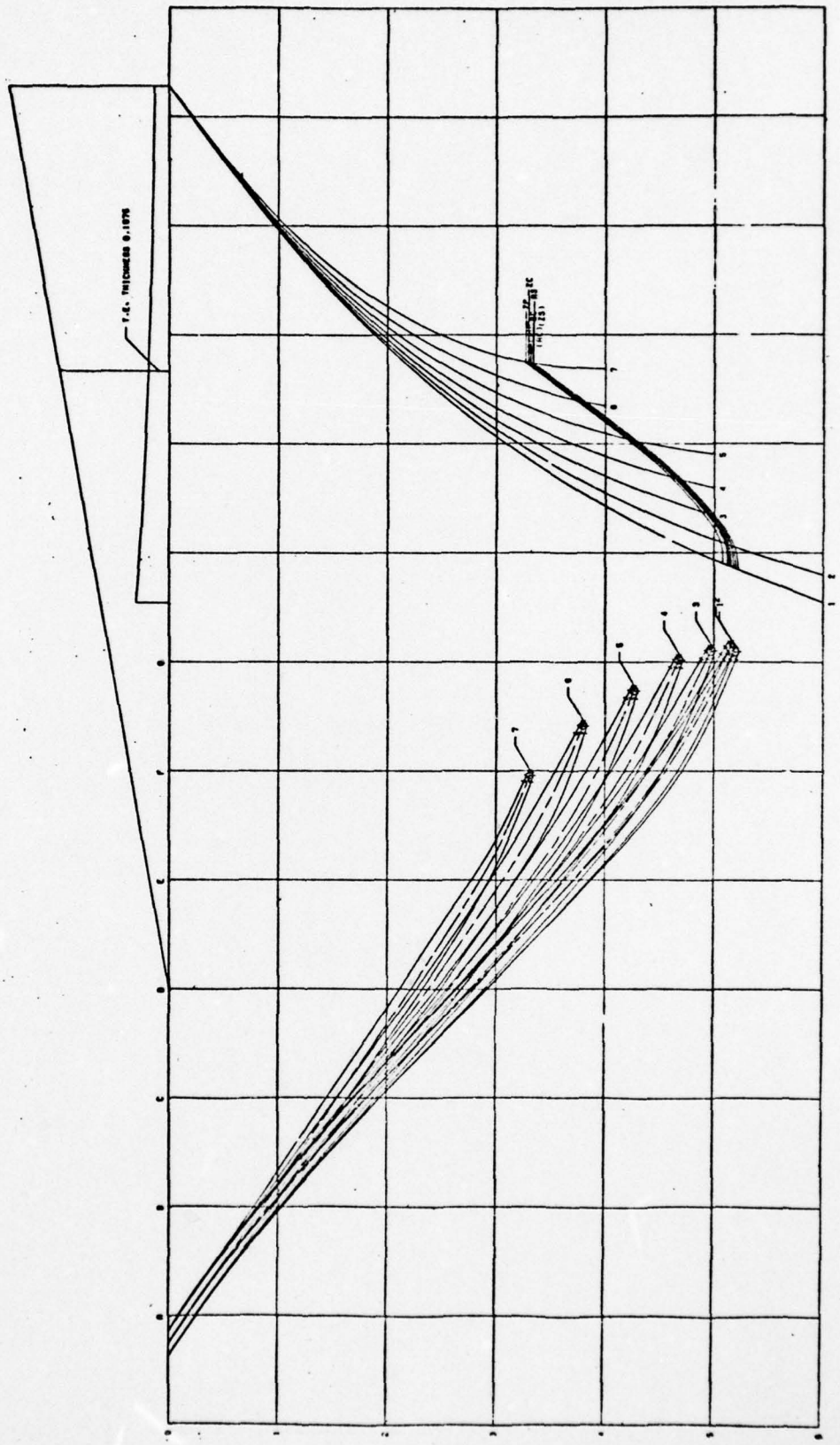

Figure E-1 - Construction of the Blade Shapes on the Conformal Grid

STREAMLINE	SURFACE	LOCATION	R-COORD	THETA-COORD	
5	SUCTION	T.E.	.165480E+02	.636614E+01	1
5	PRESSURE	T.E.	.165698E+02	.863386E+01	1
5	SUCTION		.150744E+02		2
5	PRESSURE		.163890E+02		2
5	CENTERLINE		.160950E+02		2
5	SUCTION		.153991E+02		3
5	PRESSURE		.158417E+02		3
5	CENTERLINE		.156219E+02		3
5	SUCTION		.149110E+02		4
5	PRESSURE		.153645E+02		4
5	CENTERLINE		.151373E+02		4
5	SUCTION		.144296E+02		5
5	PRESSURE		.148818E+02		5
5	CENTERLINE		.146544E+02		5
5	SUCTION		.139660E+02		6
5	PRESSURE		.144104E+02		6
5	CENTERLINE		.141862E+02		6
5	SUCTION		.135200E+02		7
5	PRESSURE		.139524E+02		7
5	CENTERLINE		.137337E+02		7
5	SUCTION		.130950E+02		8
5	PRESSURE		.135187E+02		8
5	CENTERLINE		.133000E+02		8

Table E-1 - Radial Section Coordinates for a Sample Streamline

5	SUCTION	.127086E+02	9
5	PRESSURE	.130948E+02	9
5	CENTERLINE	.128945E+02	9
5	SUCTION	.123431E+02	10
5	PRESSURE	.127125E+02	10
5	CENTERLINE	.125244E+02	10
5	SUCTION	.120255E+02	11
5	PRESSURE	.123695E+02	11
5	CENTERLINE	.121936E+02	11
5	SUCTION	.117429E+02	12
5	PRESSURE	.120621E+02	12
5	CENTERLINE	.118993E+02	12
5	SUCTION	.114874E+02	13
5	PRESSURE	.117860E+02	13
5	CENTERLINE	.116338E+02	13
5	SUCTION	.112573E+02	14
5	PRESSURE	.115348E+02	14
5	CENTERLINE	.113928E+02	14
5	SUCTION	.110519E+02	15
5	PRESSURE	.113078E+02	15
5	CENTERLINE	.111765E+02	15
5	SUCTION	.108786E+02	16
5	PRESSURE	.111051E+02	16
5	CENTERLINE	.109846E+02	16

Table E-1 (continued)

5	SUCTION	.107898E+02	17
5	PRESSURE	.109267E+02	17
5	CENTERLINE	.108140E+02	17
5	SUCTION	.105635E+02	18
5	PRESSURE	.107640E+02	18
5	CENTERLINE	.106612E+02	18
5	SUCTION	.104345E+02	19
5	PRESSURE	.106210E+02	19
5	CENTERLINE	.105250E+02	19
5	SUCTION	.103254E+02	20
5	PRESSURE	.104950E+02	20
5	CENTERLINE	.104073E+02	20
5	SUCTION	.102393E+02	21
5	PRESSURE	.103852E+02	21
5	CENTERLINE	.103081E+02	21
5	SUCTION	.101788E+02	22
5	PRESSURE	.102903E+02	22
5	CENTERLINE	.102271E+02	22
5	SUCTION	.101173E+02	23
5	PRESSURE	.102073E+02	23
5	CENTERLINE	.101594E+02	23
5	SUCTION	.100733E+02	24
5	PRESSURE	.101337E+02	24
5	CENTERLINE	.101814E+02	24

Table E-1 (continued)

SURFACE	LOCATION	R-COORD	THETA-COORD	
CENTERLINE	L.E. - B	.114937E+02	.600000E+02	22
CENTERLINE	L.E. - B	.111119E+02	.625000E+02	23
CENTERLINE	L.E. - A	.106420E+02	.650000E+02	24
CENTERLINE	L.E. - A	.100798E+02	.675000E+02	25
CENTERLINE	L.E. - A	.955669E+01	.700000E+02	26

Table E-2 - Radial Section Coordinates for a Single Leading Edge Point

BASED ON 10 BLADES, THE LIFT COEFFICIENT FOR EACH STREAMLINE IS AS FOLLOWS

STREAMLINE	RELATIVE VELOCITY RETARDATION	LIFT COEFFICIENT	CHORD LENGTH
1	1.174913	1.193372	8.854464
2	1.112297	1.152744	8.182786
3	1.036361	1.109954	8.217548
4	.960436	1.070742	8.189699
5	.888378	1.055336	7.961213
6	.825096	1.049998	7.653735
7	.777242	1.068722	7.180803

Table E-3 - Stall Evaluation for Each Streamline

5 January 1978
MCB:jep

APPENDIX F

RADIAL SECTION MODULE OUTPUT

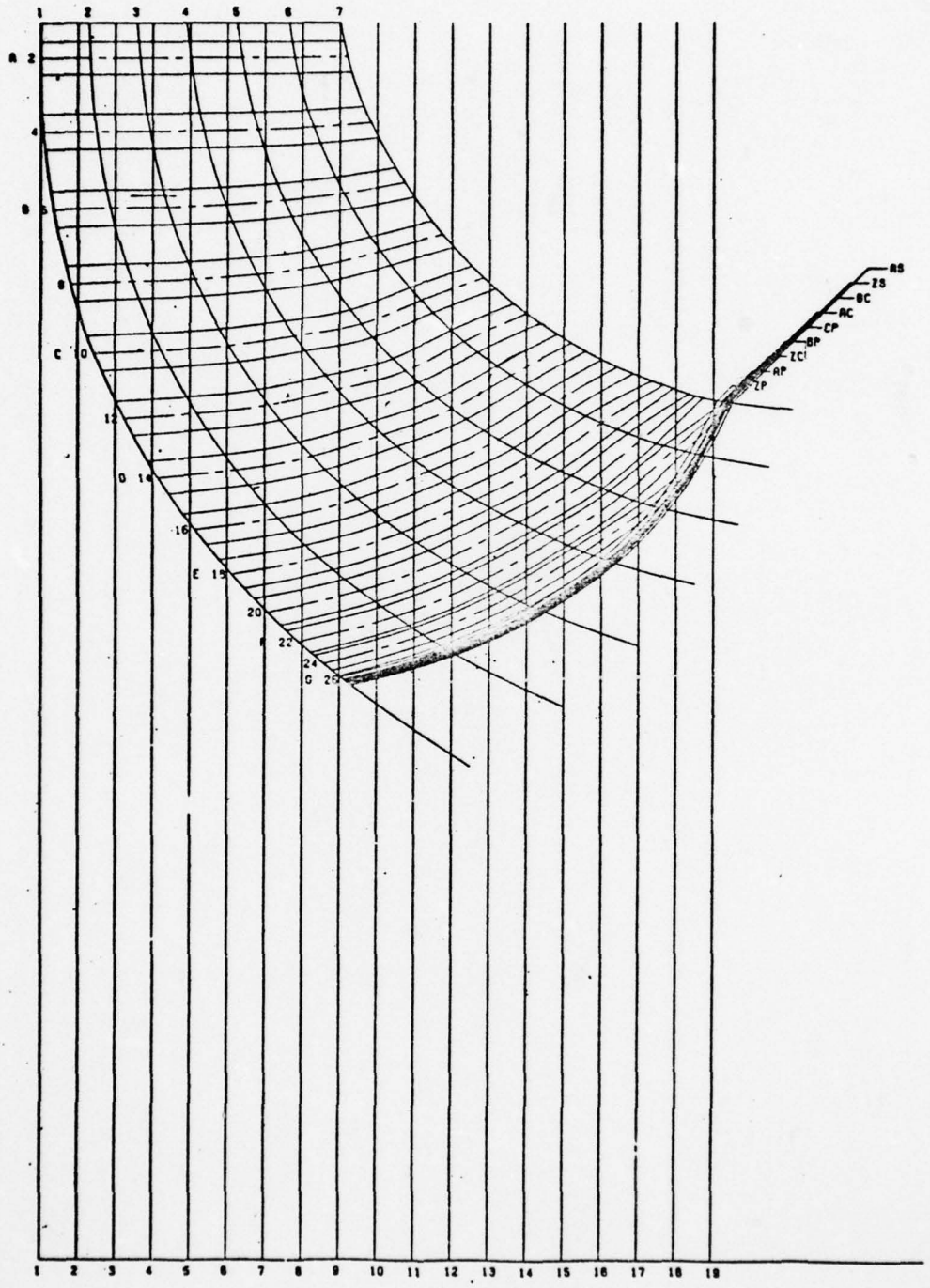

Figure F-1 - Radial Sections Transferred to the Profile View of the Impeller

BOARD SECTION	X-COORD	RADIAL SECTION	SURFACE	R-COORD	THETA-COORD
7	-10.392000	18	SUCTION	9.039794	50.000000
8	-9.892000	18	SUCTION	9.137918	50.000000
9	-9.392000	18	SUCTION	9.255173	50.000000
10	-8.892000	18	SUCTION	9.402683	50.000000
11	-8.392000	18	SUCTION	9.588262	50.000000
12	-7.892000	18	SUCTION	9.814258	50.000000
13	-7.392000	18	SUCTION	10.059123	50.000000
14	-6.892000	18	SUCTION	10.306917	50.000000
15	-6.392000	18	SUCTION	10.598331	50.000000
16	-5.892000	18	SUCTION	10.959317	50.000000
17	-5.392000	18	SUCTION	11.330156	50.000000
6	-10.892000	18	PRESSURE	9.381923	50.000000
7	-10.392000	18	PRESSURE	9.459825	50.000000
8	-9.892000	18	PRESSURE	9.552416	50.000000
9	-9.392000	18	PRESSURE	9.671467	50.000000
10	-8.892000	18	PRESSURE	9.826855	50.000000
11	-8.392000	18	PRESSURE	10.025249	50.000000
12	-7.892000	18	PRESSURE	10.249775	50.000000
13	-7.392000	18	PRESSURE	10.476441	50.000000
14	-6.892000	18	PRESSURE	10.747164	50.000000
15	-6.392000	18	PRESSURE	11.091610	50.000000
16	-5.892000	18	PRESSURE	11.420296	50.000000
17	-5.392000	18	PRESSURE	11.682084	50.000000

Table F-1 - Board Section Coordinates for a Sample Radial Section

AD-A050 187 PENNSYLVANIA STATE UNIV UNIVERSITY PARK APPLIED RESE--ETC F/G 13/10
COMPUTER-ASSISTED DESIGN OF PUMP IMPELLERS.(U)
JAN 78 M C BROPHY N00017-73-C-1418
UNCLASSIFIED TM-78-02 NL

2 OF 2
AD
A050 187

END
DATE
FILMED
3-78
DDC

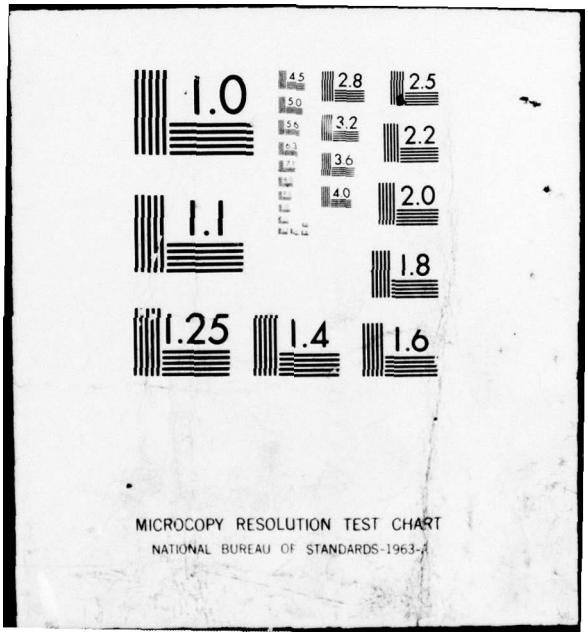
1.0
1.1
1.25
1.4
1.6
1.8
2.0
2.2
2.5
2.8
3.2
3.6
4.0
4.5
5.0
5.6
MICROCOPY RESOLUTION TEST CHART
NATIONAL BUREAU OF STANDARDS-1963-A

THE RADIUS LOCATIONS OF THE L.E. POINTS THAT ARE DETERMINED BY THE BOARD SECTIONS ARE

BOARD SECTION	L.E. POINT	R-COORD
10	RC	7.488625
11	RC	7.939734
12	RC	9.194648
13	RC	8.319340
14	RC	8.459440
15	RC	8.952024
16	RC	9.201918
17	RC	9.643918
18	RC	10.223065
19	RC	11.032692

Table F-2 - Board Section Coordinates for a Single Leading Edge Point

APPENDIX G

BOARD SECTION MODULE OUTPUT

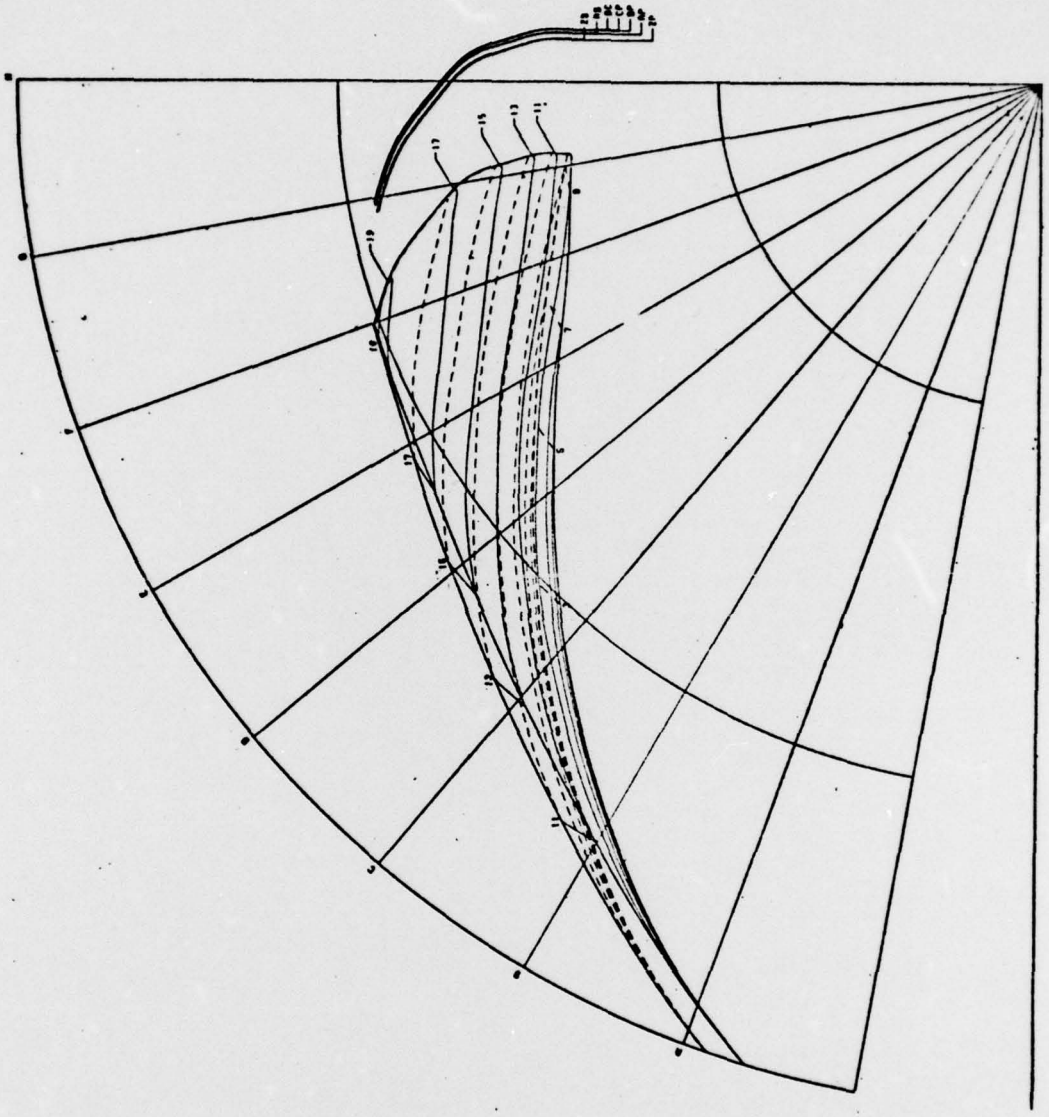

Figure G-1 - Board Sections in the Plan View of the Impeller

DISTRIBUTION LIST FOR UNCLASSIFIED TM 78-02, by M. C. Brophy, dated 5 January 1978

Commander
Naval Sea Systems Command
Department of the Navy
Washington, DC 20362
Attn: Library
Code NSEA-09G32
(Copy Nos. 1 and 2)

Naval Sea Systems Command
Attn: S. R. Marcus
Code ORD-03A
(Copy No. 3)

Naval Sea Systems Command
Attn: T. E. Peirce
Code NSEA-0351
(Copy No. 4)

Naval Sea Systems Command
Attn: Code PMS-402
(Copy No. 5)

Naval Sea Systems Command
Attn: C. Miller
Code NSEA-0331
(Copy No. 6)

Naval Sea Systems Command
Attn: A. R. Paladino
Code NSEA-0372
(Copy No. 7)

Naval Sea Systems Command
Attn: L. Benen
Code NSEA-0322
(Copy No. 8)

Naval Sea Systems Command
Attn: C. G. McGuigan
Code NSEA-03133
(Copy No. 9)

Naval Sea Systems Commmand
Attn: D. Creed
Code NSEA-03132A
(Copy No. 10)

Commander
Naval Ship Engineering Center
Department of the Navy
Washington, DC 20360
Attn: W. L. Louis
Code NSEC-6136B
(Copy No. 11)

Naval Ship Engineering Center
Attn: R. M. Petros
Code NSEC-6148
(Copy No. 12)

Naval Ship Engineering Center
Attn: J. R. Buck
Code NSEC-6136
(Copy No. 13)

Naval Ship Engineering Center
Attn: M. Hayes
Code NSEC-6110.10
(Copy No. 14)

Naval Ship Engineering Center
Attn: D. Burke
Code NSEC-6113C1
(Copy No. 15)

Commanding Officer
Naval Underwater Systems Center
Newport, RI 02840
Attn: Library
Code LA15
(Copy No. 16)

Commanding Officer
Naval Ocean Systems Center
San Diego, CA 92152
Attn: J. W. Hoyt
Code 2501
(Copy No. 17)

Naval Ocean Systems Center
Attn: J. Green
Code 254
(Copy No. 18)

DISTRIBUTION LIST FOR UNCLASSIFIED TM 78-02, by M. C. Brophy, dated 5 January 1978 (continued)

Naval Ocean Systems Center
Attn: D. Nelson
Code 2542
(Copy No. 19)

Naval Ocean Systems Center
Attn: T. Lang
(Copy No. 20)

Commander
David W. Taylor Naval Ship R&D Center
Department of the Navy
Bethesda, MD 20084
Attn: W. B. Morgan
Code 154
(Copy No. 21)

David W. Taylor Naval Ship R&D Center
Attn: J. B. Hadler
Code 1500
(Copy No. 22)

David W. Taylor Naval Ship R&D Center
Attn: G. F. Dobay
Code 1532
(Copy No. 23)

David W. Taylor Naval Ship R&D Center
Attn: R. Cumming
Code 1544
(Copy No. 24)

David W. Taylor Naval Ship R&D Center
Attn: J. McCarthy
Code 1552
(Copy No. 25)

David W. Taylor Naval Ship R&D Center
Attn: T. Brockett
Code 1544
(Copy No. 26)

David W. Taylor Naval Ship R&D Center
Attn: M. Sevik
Code 19
(Copy No. 27)

David W. Taylor Naval Ship R&D Center
Attn: B. Cox
Code 1544
(Copy No. 28)

Officer-In-Charge
Annapolis Laboratory
David W. Taylor Naval Ship R&D Center
Department of the Navy
Annapolis, MD 21402
Attn: J. G. Stricker
Code 2721
(Copy No. 29)

David W. Taylor Naval Ship R&D Center
Attn: Dr. E. R. Quandt, Jr
Code 272
(Copy No. 30)

David W. Taylor Naval Ship R&D Center
Attn: R. K. Muench
Code 2721
(Copy No. 31)

David W. Taylor Naval Ship R&D Center
Attn: J. G. Purnell
Code 2721
(Copy No. 32)

David W. Taylor Naval Ship R&D Center
Attn: M. C. Brophy
Code 2721
(Copy Nos. 33 - 40)

David W. Taylor Naval Ship R&D Center
Attn: J. V. Pierpoint
Code 2741
(Copy No. 41)

David W. Taylor Naval Ship R&D Center
Attn: J. W. Henry IV
Code 2741
(Copy No. 42)

Officer-In-Charge
Carderock Laboratory
David W. Taylor Naval Ship R&D Center
Department of the Navy
Bethesda, MD 20084
Attn: J. L. Gore
Code 1140
(Copy No. 43)

DISTRIBUTION LIST FOR UNCLASSIFIED TM 78-02, by M. C. Brophy, dated 5 January 1978 (continued)

Commander
Naval Surface Weapon Center
Silver Spring, MD 20910
Attn: Library
(Copy No. 44)

Office of Naval Research
Department of the Navy
800 N. Quincy Street
Arlington, VA 22217
(Copy No. 45)

Defense Documentation Center
5010 Duke Street
Cameron Station
Alexandria, VA 22314
(Copy Nos. 46 - 57)

Mr. George Wong
Rockedyne Div. Rockwell International
6633 Canoga Avenue
Canoga Park, CA 91304
(Copy No. 58)

Dr. George F. Wislicenus
351 Golf Court (Oakmont)
Santa Rosa, CA 95405
(Copy No. 59)

NASA Lewis Research Center
21000 Brookpark Road
Cleveland, Ohio 44135
Attn: N. Sanger
(Copy No. 60)

Dr. G. K. Serovy
Professor
Mechanical Engineering Department
Iowa State University
Ames, Iowa 50010
(Copy No. 61)

J. Horlock
Vice Chancellor
University of Salford
Salford, M5 4WT
ENGLAND
(Copy No. 62)

Dr. P. van Oossanen
Netherlands Ship Model Basin
Haagsteeg 2
P. O. Box 28
Wageningen
THE NETHERLANDS
(Copy No. 63)

Sir William Hawthorne
Whittle Turbomachinery Laboratory
Madingley Road
Cambridge
ENGLAND
(Copy No. 64)

Whittle Turbomachinery Laboratory
Attn: Library
(Copy No. 65)

Admiralty Research Laboratory
Teddington, Middlesex
ENGLAND
Attn: Dr. J. Foxwell
(Copy No. 66)

Admiralty Research Laboratory
Attn: Dr. A. Moore
(Copy No. 67)

Ken Ichirru
Hitachi Ltd.
4026 Kuji-cho
Hitachi-shi
Ibaraki-Ken, 319-12
JAPAN
(Copy No. 68)

Engineering & Research Center
Bureau of Reclamation
U. S. Department of the Interior
Room 25, Bldg. 56
P. O. Box 25007
Denver Federal Center
Denver, Colorado 80225
Attn: Henry Falvey
(Copy No. 69)

Bureau of Reclamation
Attn: Danny King
(Copy No. 70)

DISTRIBUTION LIST FOR UNCLASSIFIED TM 78-02, by M. C. Brophy, dated 5 January 1978

Dr. E. Greitzer
MS-16 United Technologies
Research Center
Silver Lane
E. Hartford, Conn. 06118
(Copy No. 71)

Mr. W. Whippen
Allis-Chalmers
Box 712
York, PA 17405
(Copy No. 72)

H. Merbt
IHAK
8012 Ottobrunn B. Munchen
Waldparkstr. 41
Munich
GERMANY
(Copy No. 73)

W. Swift
Creare Inc.
Box 71
Hanover, NH 03755
(Copy No. 74)

J. Lewis
University of Newcastle
Newcastle
ENGLAND
(Copy No. 75)

NASA Lewis Research Center
21000 Brookpart Road
Cleveland, Ohio 44135
Attn: M. Hartmann
(Copy No. 76)

Dr. R. E. Henderson
The Pennsylvania State University
APPLIED RESEARCH LABORATORY
Post Office Box 30
State College, PA 16801
(Copy No. 77)

GTWT Library
The Pennsylvania State University
APPLIED RESEARCH LABORATORY
Post Office Box 30
State College, PA 16801
(Copy No. 78)